

THE EFFECTS OF LOCAL AGGREGATES ON THE MECHANICAL
PROPERTIES OF ENGINEERED CEMENTITIOUS
COMPOSITES (ECC)

by

Michel Obied

A Thesis Presented to the Faculty of the
American University of Sharjah
College of Engineering
in Partial Fulfillment
of the Requirements
for the Degree of

Master of Science in
Civil Engineering

Sharjah, United Arab Emirates

June 2013

Approval Signatures

We, the undersigned, approve the Master's Thesis of Michel Issa Obied.

Thesis Title: The Effects of Local Aggregates on the Mechanical Properties of Engineered Cementitious Composites.

Signature

Date of Signature
(dd/mm/yyyy)

Dr. Adil K. Al-Tamimi
Professor of Civil Engineering
Thesis Advisor

Dr. Mohamed Maalej
Vice Dean, College of Engineering at the University of Sharjah
Thesis Committee Member

Dr. Rami A. Hawileh
Associate Professor, Department of Civil Engineering
Thesis Committee Member

Dr. Farid H. Abed
Associate Professor, Department of Civil Engineering
Thesis Committee Member

Dr. Sameh M. El-Sayegh
Head, Department of Civil Engineering

Dr. Hany El Kadi
Associate Dean, College of Engineering

Dr. Leland T. Blank
Interim Dean, College of Engineering

Dr. Khaled Assaleh
Director of Graduate Studies

Acknowledgements

I would like to acknowledge my advisor, Dr. Adil Al-Tamimi, Professor of Civil Engineering, for his supervision, motivation, and guidance throughout the research program. Also, I would like to thank my committee members, Dr. Mohamed Maalej, Dr. Rami Antoun Hawileh, and Dr. Farid Abid for their feedback, encouragement, and support of this research program. Finally, I would like to thank Eng. Arshi Faridi and Eng. Mohammad Ansari for their support during the experimental stage of the research program which includes different aspects such as preparing and controlling the ECC specimen and conducting tests in accordance with ASTM standards as well as controlling the testing machines.

Abstract

Engineered Cementitious Composites (ECC) are a class of ultra-ductile fiber reinforced cementitious composites characterized by a strain hardening behavior and a high strain capacity when subjected to tensile loading. ECC integrates micromechanical models and fracture mechanics principles in the design concept which makes it an engineered material. These features promote ECC as a promising material for a wide range of applications which include repair of structures, and resistance to seismic activity, impacts, and blasts. However the high initial cost of the material which is three times the cost of conventional concrete hinders the widespread use of ECC. Also, the high carbon footprint and the high cement volume can be a potential problem for the environment. Therefore this research sought to reduce the cement volume by producing ECC with aggregates and producing it at an Aggregate to Binder ratio of 0.8. This means the new non-standard ECC has twice as much aggregate as can be found in standard ECC. ECC with aggregates is expected to perform better than standard ECC in terms of drying shrinkage, creep, workability, strength, and cost, while still preserving all the good mechanical performance of standard ECC. There is however a decrease in strain capacity from 5% to 2%. Other researchers also faced this decrease in strain capacity when investigating ECC with aggregates. Yet, this research provides an even better version of ECC with aggregates which has a compressive strength of about 82 MPa and a tensile strength of 8 MPa on average. Furthermore, the fiber / matrix interfacial bond (τ) was estimated to be around 1.4 MPa. The high estimated bond value was a result of using a special technique to increase the strength and the particle packing of the ECC matrix. Moreover, by using local materials available in the UAE, this research proved that aggregates in the UAE are suitable for making ECC. Finally, this research attempted to use Ultra-fine fly ash in order to regain strain capacity and to enhance the greenness and the workability of the material. Results of the current research will open the door into a vast range of research regarding ECC with aggregates.

Search Terms: *[Engineered Cementitious Composites, Aggregates, Mechanical Performance, Interface, Bond, Matrix Toughness, Fibers, Ultra-fine fly ash]*

Table of Contents

Abstract.....	6
List of Figures	9
List of Tables.....	11
Nomenclature	12
List of Symbols	13
Chapter 1: Introduction	14
1.1 Background & Motivation:	14
1.2 History of Fiber Reinforced Concrete (FRC):.....	14
1.3 Engineered Cementitious Composites:	15
1.4 Problem Statement:	16
1.4.1 Research Objectives:.....	17
1.4.2 Scope of Work:	17
1.4.3 Research Significance:.....	18
Chapter 2: Literature Review.....	20
2.1 Micromechanics Design Theory:	20
2.1.1 Micromechanics & Fiber Bridging:.....	20
2.1.2 Steady State & Multiple Cracking:.....	22
2.1.3 Fracture Energy & Toughening Mechanisms:.....	24
2.1.4 Criteria for Strain Hardening:	26
2.2 Micromechanics Summary:.....	29
2.3 Tailoring Individual Micromechanics Parameters:.....	31
2.3.1 Fiber:.....	31
2.3.2 Matrix:.....	33
2.3.3 Interface:	35
2.4 Effect of Aggregates on ECC:.....	42
2.5 Rheological Control of ECC:	43
2.6 Effect of Fly Ash on ECC:	43
2.7 Effect of Blast Furnace Slag on ECC:.....	46
2.8 Effect of Silica Fume on ECC:.....	48
Chapter 3: Experimental Program & Materials Characterization	49
3.1 Experimental Program:	49
3.1.1 ECC Mixture design:	49

3.1.2	Mixing procedure and curing:.....	50
3.1.3	Uniaxial Tensile Tests & Compressive Tests:.....	52
3.2	Materials Characterization:	53
3.2.1	Aggregates:	53
3.2.2	Fibers.....	56
3.2.3	Cement	57
3.2.4	High Range Water Reducer	57
Chapter 4: Test Results and Discussion:		58
4.1	Test Results:	58
4.1.1	Compressive Strength:	58
4.1.2	Tensile Strength & Tensile Strain:.....	59
4.1.3	The effect of ultra-fine fly ash on ECC:	63
4.1.4	Comparison with data in the literature:.....	64
4.1.5	Analytical Predictions:.....	67
4.2	Failure modes and possible errors affecting the results:	69
4.2.1	Uniform distribution of fibers in the matrix:	69
4.2.2	Aggregate size:.....	69
4.2.3	Machine Gripping:	70
4.2.4	Testing Errors:	72
Chapter 5: Summary, Conclusions, and Future Research:		73
5.1	Summary	73
5.2	Conclusions & Future Research:.....	74
5.2.1	Conclusions:.....	74
5.2.2	Discussion of Conclusions and Future Research:.....	75
Works Cited.....		77
Appendix.....		80
Vita		83

List of Figures

Figure 1: The link between material constituents, crack bridging property and composite ductility [13].	20
Figure 2: σ - δ curve and the concept of complementary energy	21
Figure 3a: Low complementary energy in comparison to crack tip toughness results in Griffith type cracking [13].	23
Figure 3b: High complementary energy results in a flat crack propagation which leads to the phenomenon of multiple cracking [13].	23
Figure 4: Fracture energy measure on and off crack plane of spectra (polyethylene) ECC. ...	26
Figure 5: σ - δ curve and the concept of complementary energy (J_b') [20].	28
Figure 6: Micromechanics as a tool for microstructure tailoring [5].	30
Figure 7a: Individual effects of strength criterion and energy criterion on the critical fiber volume fraction at different interfacial bond strength [20].	32
Figure 7b: Combined effect of energy and strength criteria on the critical volume fraction at different bond strength [20].	32
Figure 8a: Individual effects of strength criterion and energy criterion of two types of fibers on the critical fiber volume fraction at different interfacial bond strength [20].	33
Figure 8b: Combined effect of energy and strength criteria of two types of fibers on the critical volume fraction at different bond strength [20].	33
Figure 9: Variation of matrix fracture toughness with interfacial bond, strength, and critical fiber volume fraction.	34
Figure 10: Matrix toughness variation with sand/cement ratio for two water/binder ratios [23].	35
Figure 11: General fiber pullout test profile showing slip hardening, slip softening and constant friction [25].	36
Figure 12: Effect of plasma treatment on the frictional bonds of polyethylene ECC.	38
Figure 13: Pullout tests of plasma treated and non-treated polyethylene fibers [26].	39
Figure 14: Pullout tests of plasma treated and non-treated polypropylene fibers [27].	41
Figure 15: Chemical bond variation with increasing fly ash content [7].	45
Figure 16: Slip hardening coefficient variation with increasing fly ash content [7].	45
Figure 17: Frictional bond variation with increasing fly ash content [7].	46
Figure 18: Fiber dispersion tank.	51
Figure 19: Tensile test layout [2].	53
Figure 20: Deformed ECC cube.	59
Figure 21: Average 14 days tensile strength of all the tested ECC mixtures.	59
Figure 22: Average 14 days tensile strain of all the tested ECC mixtures.	60

Figure 23: Seven days tensile strain of all the tested ECC mixtures.	61
Figure 24: Plot of tensile strain variation with interfacial frictional bond.	62
Figure 25: Tensile stress versus strain diagrams from previous research on ECC made with aggregates (dolomitic limestone) [24].	65
Figure 26: Tensile stress versus strain diagrams from previous research on ECC made with aggregates (gravel sand) [24].	65
Figure 27: Tensile stress versus strain diagrams of several ECC samples in the current research.	66
Figure 28: 14 days tensile strain results of individual ECC samples tested in this research...	67
Figure 29: PSH Energy Index for all possible matrix toughness and frictional bond values.	68
Figure 30: Bad samples (cracks are seen next to the grips only).	70
Figure 31: Good samples (tiny micro-cracks distributed over the sample length).	70
Figure 32: Good sample top view.	71
Figure 33: Good sample top view (zoomed in at the cracks area).	71

List of Tables

Table 1: Summary of toughening mechanisms in cement based composites	25
Table 2: Summary of recommended pseudo strain hardening indices.	32
Table 3: Typical frictional bond values of virgin and treated polyethylene fibers [26].....	37
Table 4: Effect of fiber oiling on the interfacial properties and complementary energy of ECC [6].....	40
Table 5: Effect of oiling agent on experimentally measured mechanical properties of ECC [6].	40
Table 6: Typical size distribution of silica sand	42
Table 7: Effect of silica fume addition to ECC matrix on the interfacial frictional bond.....	48
Table 8: Mix designs.....	50
Table 9: Particle size distribution of silica sand and dune sand.....	54
Table 10: Particle size distribution of crushed limestone.	55
Table 11: Specific gravity, absorption, and moisture content test results for the local materials.	55
Table 12: Mortar flow test results of varying aggregate ratios.	56
Table 13: Polyethylene fiber specifications.	57
Table 14: Compressive strength results of mortar and ECC mixtures.....	58
Table 15: HRWR dosage with increasing UFFA content.	63
Table 16: Tensile strain and tensile strength data for all the samples at 7 days and 14 days...	80
Table 17: Average tensile strain and tensile strength for all the samples at 7 days and 14 days.	80
Table 18: Calculation of the crack tip toughness (J_{tip}) using the possible matrix toughness interval (0.1 to 1).	80
Table 19: Calculation of the complementary energy J_b' using a chosen frictional bond interval (0.6 to 2.1).....	81
Table 20: All possibilities of J_b' / J_{tip} for the chosen intervals of the frictional bond and the matrix toughness; it was used to plot figure 27.	82

Nomenclature

ASTM – American Society for Testing and Materials

BFS – Blast Furnace Slag

CEM – Cement

ECC – Engineered Cementitious Composites

FRC – Fiber Reinforced Concrete

HPFRCC – High Performance Fiber Reinforced Cementitious Composites

HRWR – High Range Water Reducer

HSC – High Strength Concrete

HVFA ECC – High Volume Fly Ash Engineered Cementitious Composites

LVDT – Linear Variable Differential Transformer

LWC – Light Weight Concrete

MAS – Maximum Aggregate Size

NSC – Normal Strength Concrete

OPC – Ordinary Portland Cement

PE – Polyethylene

PP – Polypropylene

PSH – Pseudo Strain Hardening

PVA – Poly-vinyl Alcohol

SHCC – Strain Hardening Cementitious Composites

UFFA – Ultra Fine Fly Ash

UAE – United Arab Emirates

VMA – Viscosity Modifying Agent (Viscosity Modifying Admixture)

W/B – Water to Binder Ratio

W/C – Water to Cement Ratio

List of Symbols

A_0 – Initial Matrix Flaw Size Distribution

D_f – Fiber Diameter

E_c – Composite Elastic Modulus

E_f – Fiber modulus of elasticity

E_m – Matrix Elastic Modulus

G_d – Fiber/Matrix Interface Chemical Bond

g – Snubbing factor

J_b' – Complementary Energy

J_{tip} – Crack tip toughness

K_m – Matrix Toughness

L_f – Fiber Length

V_f – Fiber Volume fraction

β – Slip Hardening Coefficient

δ – Crack Opening (displacement)

σ_{cu} – Maximum fiber bridging stress

σ_{fc} – Matrix First Cracking Strength

σ_{fu} – Fiber Tensile Strength

τ – Fiber/Matrix Interface Frictional Bond

Chapter 1: Introduction

1.1 Background & Motivation:

Fiber reinforced concrete is a type of concrete which contains fibrous materials to increase the energy absorption capacity (toughness) and the load carrying capacity (strength) of the material in order to provide a better structural performance. There are many types of fibers which can be used in concrete such as steel fibers, glass fibers, synthetic fibers, carbon fibers etc... These fibers come with different aspect ratios (length to diameter ratio) and different sizes such as micro or macro fibers. Furthermore, fibers used in concrete can be uniformly distributed continuous fibers or randomly distributed discontinuous fibers. The wide variety of fiber types, shapes, and processing methods available for use in fiber reinforced concrete corresponds to the wide range of applications available for this type of concrete. For Instance, short discontinuous randomly distributed fibers are usually used in Bulk Structures while continuous fiber meshes are used in thin sheets [1]. An important property in fiber reinforced concrete is the fiber volume fraction. In FRC, the fiber volume fraction is the amount of fibers added to a cement matrix which is usually represented by a fraction of the volume of the final concrete product. Generally, a high fiber volume fraction translates into better FRC performance however this high fiber volume FRC is hindered by the special processing requirements and high production cost [2]. Therefore need arises for a material having a low fiber volume fraction for ease of processing while maintaining the high performance of high fiber volume FRC. This material was developed at the University of Michigan by Dr. Victor Li and was called Engineered Cementitious Composites (ECC).

1.2 History of Fiber Reinforced Concrete (FRC):

Historically speaking, people started using fibers from ancient times as in Finland where natural fibers were used to make clay pots. Also, in Egypt people used straw to make mud bricks. Although people were using different types of fibers for various purposes, the use of fibers in concrete did not start until the early 1900s as asbestos fibers were the first to be used in concrete. However, the modern development and addition of steel fibers into concrete started around the early 1960s [1]. Then in the 1970's polymeric fibers were developed and people started using

them in concrete [1]. Even though, attempts to incorporate glass fibers into concrete failed in the 1930's, developments in glass fibers made them possible by the early 1980's. Later, in the 1990's, carbon fibers became common in concrete [1]. Since fibers are good in taking tensile loads, they have found good use in concrete which is a material that lacks appropriate strength under tension. The relatively low tensile strength of concrete makes it prone to cracking when tension loaded. Therefore besides using fibers to improve the tensile properties of concrete, fibers were also used to control cracks. Nowadays, the addition of fibers to concrete can provide the material with higher fracture toughness and thus more energy absorbing capacity. This feature is highly desirable in concrete designed to resist impact loads and seismic activity. Also, fibers were able to provide concrete with a much higher strain capacity. This feature is extremely important as it changes the failure mode of the material from a quasi-brittle one to a semi ductile failure behavior.

1.3 Engineered Cementitious Composites:

Engineered cementitious composites (ECC) are a class of ultra-ductile fiber reinforced cementitious composites. They were developed at the University of Michigan during the early 1990's. ECC has undergone major evolution in both materials development and the range of emerging applications. Engineered cementitious composites (ECC) also called bendable concrete are an easily molded mortar-based composites reinforced with specially selected short random fibers, usually polymer fibers [3]. Unlike regular concrete or FRC, ECC has a strain capacity in the range of 3–6%, compared to 0.1 % for ordinary Portland cement (OPC). ECC therefore acts more like a ductile metal than a brittle glass (as does OPC). Some researchers defined ECC as a unique class of high performance fiber reinforced cementitious composites (HPFRCC) with significant strain hardening behavior under tension [4]. It is also considered a strain hardening cementitious composite (SHCC) due to its ductile failure mode. ECC imparts ductility and durability to the structure due to high strain capacity and low crack width. The large strain is contributed by sequential development of multiple cracks instead of continuous increase of crack opening. The associated high fracture toughness and controlled crack width (typically below 100um) makes ECC an ideal material to improve serviceability and durability of infrastructures. Material engineering of ECC is constructed on the paradigm of the

relationships between material microstructures, processing, material properties and performance where micromechanics is highlighted as the unifying link between composites mechanical performance and material microstructure properties. ECC has a variety of unique properties, including tensile properties superior to other fiber-reinforced composites, ease of processing on par with conventional cement, the use of only a small volume fraction of fibers 2% and small crack width [4]. These properties are due largely to the interaction between the fibers and cementing matrix, which can be custom-tailored through micromechanics design. Essentially, the fibers create many micro cracks with a very specific width, rather than a few very large cracks as in conventional concrete. This allows ECC to deform without catastrophic failure. The material has been successfully applied to dam repair, bridge deck overlays, coupling beams in high rise buildings and other structural elements and systems.

1.4 Problem Statement:

ECC is a relatively new material with very promising characteristics and performance however it has its own limitations. The first and main problem encountered when trying to replicate ECC specimens is the lack of standard design guidelines. That is due to the fact that the material is still new and is under extensive research. This makes data available on ECC lacking some consistency and therefore more research is needed to confirm previous results. Another challenge is to design ECC with local materials available in the UAE such as limestone powder, dune sand, or other fine aggregates in order to evaluate their effect on the mechanical performance of the composite. It is important to study the effects of using local materials since ECC is usually designed with specific ingredients in mind including a special type of sand (silica sand) and certain fiber types (Polyethylene or PVA). Furthermore, the high initial investment cost of ECC compared to normal concrete is a major problem limiting the materials potential. The high cost is due to the high cement content of this composite and the high cost of the polyethylene fiber which is considered the main fiber used in ECC [5] [6]. Moreover, the high cement content can cause shrinkage and has a high carbon footprint. However, this problem is currently being addressed by other researchers who successfully replaced a large portion of cement in ECC by fly ash [7] [8]. However, if ECC can be made with aggregates and with twice the amount of aggregates found in previous ECC mix designs, then its cost, its material greenness and its mechanical properties can be enhanced. Besides that, trying to add ultra-fine

fly ash (UFFA) to ECC mixtures was not yet investigated. Also, even though the main reason for introducing PVA fibers to ECC was to improve the cost of the composite, since they are about 8 times cheaper than polyethylene, the PVA fibers are not good under varying strain rates and have their own limitations due to their hydrophilic nature [5] [6] [9]. Therefore the first target of this research is to develop ECC with local materials using polyethylene fibers. The second goal is to use different techniques to enhance the mechanical properties of aggregate containing ECC. The third goal will be to investigate the effect of ultra-fine fly ash on fresh and hardened ECC. The addition of ultra-fine fly ash and the use of a mortar flow table technique to be discussed later will make the fresh ECC mixture more workable and therefore decrease the required chemical admixture dosage which saves some money and also making the material more sustainable.

1.4.1 Research Objectives:

1. Design ECC mixtures using local materials available in the UAE.
2. Enhance the mechanical properties of aggregate containing ECC by using several methods such as altering mix ingredients and ratios and by enhancing the particle packing through a mortar flow table technique.
3. Investigate the effect of ultra-fine fly ash on the fresh and hardened properties of ECC.
4. Enhance the material greenness by using a 0.8 aggregate to binder ratio which decreases the volume of cement in ECC samples.
5. Reduce the cost of producing ECC by adding larger sized aggregates and by using an aggregate to binder ratio of 0.8 which reduces the cement volume as well as the HRWR dosage due to the increased workability.
6. Evaluate and analyze results to characterize the effects of mix ingredients, mix design proportions such as (A\B and W\B), and ultra-fine fly ash on the mechanical performance of ECC.

1.4.2 Scope of Work:

This research investigates the development of Engineered Cementitious Composites with local materials available in the UAE. In order to do that, knowledge of standard and common practices in developing ECC is needed. Thus an extensive

literature review mentioning the findings of several researches regarding individual factors affecting the performance of ECC was conducted. Factors such as aggregate type and ratio, supplementary cementitious materials, and micromechanics design principles were reviewed. Then, based on the review, a series of mix designs with local aggregates were prepared to investigate the effect of local materials on the mechanical performance of the composite. Then, mortar flow table tests were used to find the optimum ratio of aggregates to be used in mix designs. This ratio is expected to increase the performance of ECC as the optimum ratio increases the particle packing of the mixes. After that, ultra-fine fly ash was added to the ECC mixtures to investigate its effect on the fresh and hardened properties of ECC. Finally, the results of previous research were compared to the results of this research in order to draw conclusions. It should be noted that the study of the effect of varying the fiber volume is out of the scope of this research and therefore was held constant in all the ECC mixtures prepared.

1.4.3 Research Significance:

This project is unique since it studies the effect of several factors on a relatively new material. Also, this project is unique since it takes place in a country that had significantly many construction projects taking place during the past ten years. The huge number of buildings and projects constructed during the past 20 years will require rehabilitation in the near future. Here comes the role of ECC as a potential repair material. Therefore it is important to be able to develop ECC with local materials and to understand what factors affect the performance of this composite. Also this study investigates the use of aggregates in ECC which if possible will enhance the greenness and the mechanical properties of the material as well as reduce its cost by a small amount. Moreover, it investigates the effect of a new type of fly ash (UFFA) on the performance of ECC. The fact that no studies of the effect of UFFA on ECC are available makes this research even more significant. Besides that, in the UAE corrosion of steel is considered a very widespread and dangerous problem hindering the life span and performance of built structures. ECC having a very tight crack width and expansion ability that prevents spalling is considered suitable for addressing the problem of reinforcing steel corrosion. Furthermore, ECC is a material that has a high damage tolerance capacity and can withstand impact loads up to 17 times more than concrete [10] [11]. This makes ECC a suitable material to protect

important buildings such as government and military buildings against possible terrorist attacks.

Chapter 2: Literature Review

2.1 Micromechanics Design Theory:

2.1.1 Micromechanics & Fiber Bridging:

Micromechanics relate macroscopic composite properties to the microstructure of the materials forming the composite, and it is considered the backbone of the material design theory. ECC has a tensile strain capacity of about 7 percent which is almost 700 times larger than normal reinforced concrete [12]. Therefore in order to achieve this high ductility and strain, it is essential to understand the micromechanics design theory of this composite material (matrix toughness, fiber strength, multiple cracking, bridging law etc...). Also, micromechanics can be used as an analytical tool for composite optimization enabling high performance along with easy processing and minimum fiber content [13]. As well as providing a systematic approach for material tailoring which minimizes the number of trial and error experiments and increases the development speed of ECC [13]. Consequently, the micromechanics based design concepts make ECC an engineered material rather than being just a composite with high ductility [13].

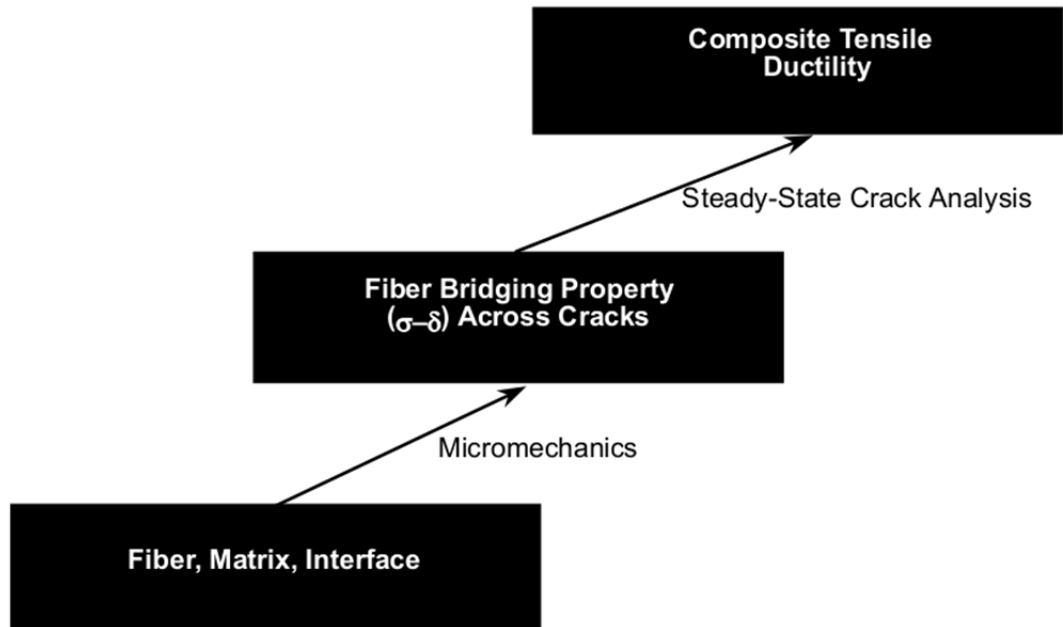


Figure 1: The link between material constituents, crack bridging property and composite ductility [13].

In FRC, ECC, or any cementitious composite, the fiber bridging property across a matrix crack (σ - δ curve) is considered the most important property of the

material. This σ - δ curve is the average tensile stress (σ) transmitted across a crack with uniform crack opening (δ) [13]. As shown in figure above, the bridging property provides a link between the material constituents (fiber, matrix, and interface) and the composite tensile ductility. “The σ - δ curve shown in the figure below can be thought of as a spring law describing the behavior of non-linear spring connecting the opposite surfaces of a crack, representing the averaged forces of the bridging fiber acting against the opening of the crack when the composite is tension loaded” [13]. Moreover, as will be described later, fiber bridging plays a role in the load bearing capacity and some of the energy absorption capacity of ECC. Besides that, micromechanics analysis shows that high bridging strength σ_{cu} and large complementary energy C are beneficial for strain-hardening of ECC [4].

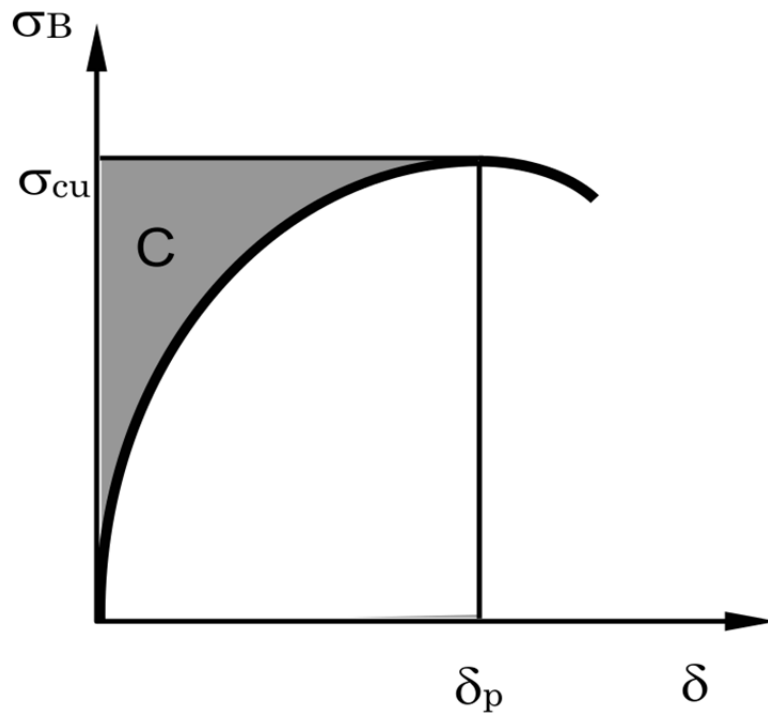


Figure 2: σ - δ curve and the concept of complementary energy. (shaded area labeled C which will be called J_b later) [13].

The σ - δ curve is considered important for ECC analysis and design because, as will be seen later, the criteria for strain hardening are related to the complementary energy (C) and bridging strength (σ_{cu}) derived from the σ - δ curve. Furthermore, a fiber bridging relationship $\sigma(\delta)$ or fiber bridging law developed for ECC can be used as a model to plot the curve is described by the following [12]:

$$\sigma(\delta) = \begin{cases} \sigma_0 [2(\delta/\delta_0)^{1/2} - (\delta/\delta_0)] & \text{for } \delta \leq \delta_0 \\ \sigma_0 (1 - 2\delta/L_f)^2 & \text{for } \delta_0 \leq \delta \leq L_f/2 \\ 0 & \text{for } L_f/2 \leq \delta \end{cases} \quad (2.1)$$

$$\text{Where } \sigma_{cu} = \sigma_0 = \frac{g\tau V_f L_f}{2d_f} \quad (2.2)$$

$$\& \delta_p = \delta_0 = \frac{\tau L_f^2}{E_f d_f (1+\eta)} \quad (2.3)$$

As a note, the above bridging law does not account for two way fiber pullout or the cook-gordon effect [14]. A newer more accurate bridging law by [14] has been derived for ECC however the discussion of the newer law is not of the scope of this paper. As can be seen from the above equations and as mentioned by [15], the shape of the σ - δ curve is controlled by the fiber volume fraction (V_f), diameter (d_f), length (L_f), strength and modulus of elasticity (E_f), in addition to interfacial chemical and frictional bonds (G_d and τ).

2.1.2 Steady State & Multiple Cracking:

Steady-state cracking is defined as crack extension at constant crack width under constant loading independent of crack length [16]. This type of cracking is usually called a flat crack. Steady state cracking is very desirable for strain hardening in discontinuous random fiber reinforced composites. When the applied load exceeds the matrix cracking strength, also known as the first cracking strength, two different scenarios can occur: a Griffith crack or a Steady State (flat) crack. The first scenario occurs when the complementary energy (C), described in the previous section, is small where the crack will behave like a Griffith crack as shown in figure below [13]. As the crack propagates, unloading of the fiber initiates at the middle of the crack where the opening is maximum ($\delta_m > \delta_p$) [13]. Therefore, the fibers will rupture or be pulled out of the matrix depending on the interface strength [4]. Consequently, the composite will fail with a reduced load carrying capacity which leads to the tension softening behavior of FRC. However, if the complementary energy (C) is large, the second scenario will occur where the crack will remain flat as it propagates so that the steady state cracking opening is less than the maximum bridging stress opening ($\delta_{ss} < \delta_p$) [13]. When a flat crack occurs, the bridging fibers are still able to sustain the load and pass it back from the crack plane to the matrix without rupturing or diminishing

[16]. Furthermore, the load transferred back to the matrix will cause the initiation of another crack from a different matrix defect site. Repetition of this steady state cracking process is called the phenomenon of multiple cracking which in turn leads to strain hardening of the composite. Moreover, additional load could be applied until the post crack strength or maximum bridging stress (the maximum value of σ - δ curve) is reached. More on steady state crack propagation and multiple cracking can be found in [4].

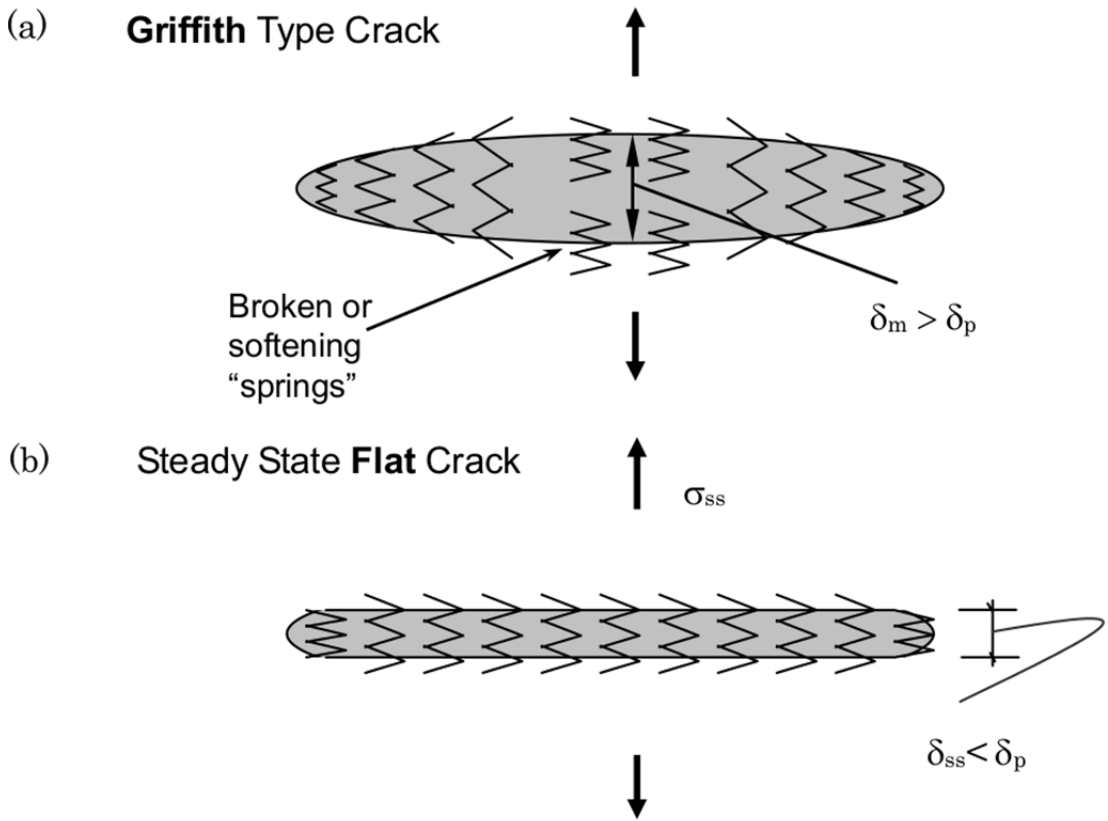


Figure 3a: Low complementary energy in comparison to crack tip toughness results in Griffith type cracking [13].

Figure 3b: High complementary energy results in a flat crack propagation which leads to the phenomenon of multiple cracking [13].

Research shows two important criteria for achieving steady state cracking. 1) Stress at the midpoint of the crack must be equal to the first crack strength. 2) The crack opening displacement at the midpoint of the crack δ_m must be less than the displacement δ_p corresponding to maximum bridging stress [4]. The equation for critical opening δ_p is given as

$$\delta_p = \frac{\tau L_f^2}{E_f d_f (1 + \eta)} \quad (2.4)$$

This equation will be used later in the analysis of the strain hardening criteria of ECC.

2.1.3 Fracture Energy & Toughening Mechanisms:

Many researchers found out that ECC failed in a completely different mode as compared to other cementitious composites. Fracture failure in cement pastes is very brittle, and fracture in concrete and FRC is quasi brittle whereas in the case of ECC, the fracture is quasi-ductile [17]. This is due to the effects of two toughening mechanisms occurring in ECC: fiber bridging and multiple micro-cracking [18]. The table below shows the various toughening mechanisms occurring in NSC, LWC, HSC, FRC and ECC and their contribution to the toughness in composites [18]. It is clear that the toughening mechanisms such as multiple micro-cracking and fiber bridging (pullout and debonding) have the highest contribution to composite toughness when compared to cement pastes (x1000 and x250 respectively). Furthermore, it is worth noting that multiple micro-cracking is a unique behavior of Engineered Cementitious Composites and that this toughening mechanism does not occur in NSC, LWC, HSC, or FRC [19]. This is the main reason for ECC to beat FRC in composite fracture toughness and in possessing a strain hardening behavior since only fiber bridging occurs in FRC. Besides that, the increase in fracture toughness of the composite brings about a high energy dissipation capability and thus makes the material much more damage tolerant. The total energy dissipated by fracture can be divided into two components: energy dissipated by fiber bridging processes occurring on the main fracture plane (J_b) and energy dissipated by micro-cracking processes occurring off the crack plane (J_m) [17].

Table 1: Summary of toughening mechanisms in cement based composites [18].

<i>Toughening mechanism</i>	<i>Location</i>	<i>Toughness increase over cement</i>	<i>Detection technique</i>	<i>Remark</i>
Microcrack shielding	Frontal	10–20% ⁴⁷ up to 29% ³⁶	X-Ray ^{24,41} Stereomicroscopy ⁷² 3-D AE ²⁵ Laser holography ²⁸ Quantitative AE ³³ SEM ⁶⁷ Laser interferometry ²⁹	Concrete MPZ \approx 25 mm ⁶⁸ HCP MPZ \approx 50 μ m ⁶⁷
Crack deflection	Crack tip	10–20% ⁴⁷ up to 27% ³⁶	SEM during loading ^{38,42} X-ray ²⁴	
Crack trapping	Crack tip	60–90% ⁴⁶	Should be detectable by dyed epoxy impregnation technique	Not yet observed in cement based materials, but expected in HSC
Crack face pinning	Wake	15–40% ⁴⁶	Should be detectable by dyed epoxy impregnation technique	Not yet observed in cement based materials, but expected in HSC
Aggregate/ligament bridging	Wake	\sim 130% (over mortar) ⁶⁰	SEM during loading ^{38,42} Long distance microscope ⁵³ Epoxy impregnation and UV photography ⁵³ X-ray ²⁴	Concrete FPZ > 50 mm, ⁶⁸ 20–40 mm, ²⁹ 20–30 mm, ³⁰ 30–40 mm, ⁸⁴ 12–43 mm, ⁸⁵ 70 mm, ²⁵ 29 mm long and 20 mm wide ²⁴
Fiber debonding	Wake-frontal		SEM during loading ⁴² Moiré interferometry ⁸⁶	
Fiber pull-out	Wake	Up to 250 \times ⁸⁷	SEM during loading ⁴²	Bridging zone in cm to m scale depending on fiber length ⁸⁸
Multiple micro-cracking	Frontal	Up to 1000 \times ^{89–90}	Regular photography during loading ^{89–90}	Volumetric, covers over 1000 cm ² on specimen surface ⁸⁹

The figure below shows the experimentally measured on and off crack plane fracture energy. The on crack plane fracture energy caused by fiber bridging J_b has been determined from the area under the descending branch of a uniaxial tensile test. The off crack plane fracture energy J_m has been determined by subtracting the bridging energy J_b from the total composite fracture energy J_c which was calculated based on the J-integral technique [17]. It is seen that the off-crack plane fracture energy is non-existent when the fiber volume fraction is below the critical value V_f critical. Above V_f critical however the off crack plane fracture energy caused by micro-cracking increases and eventually exceeds that of the fiber bridging energy consumed on the crack plane. It is clear that the ductile fracture mode is closely associated with the condition of pseudo strain hardening from the above discussion [17].

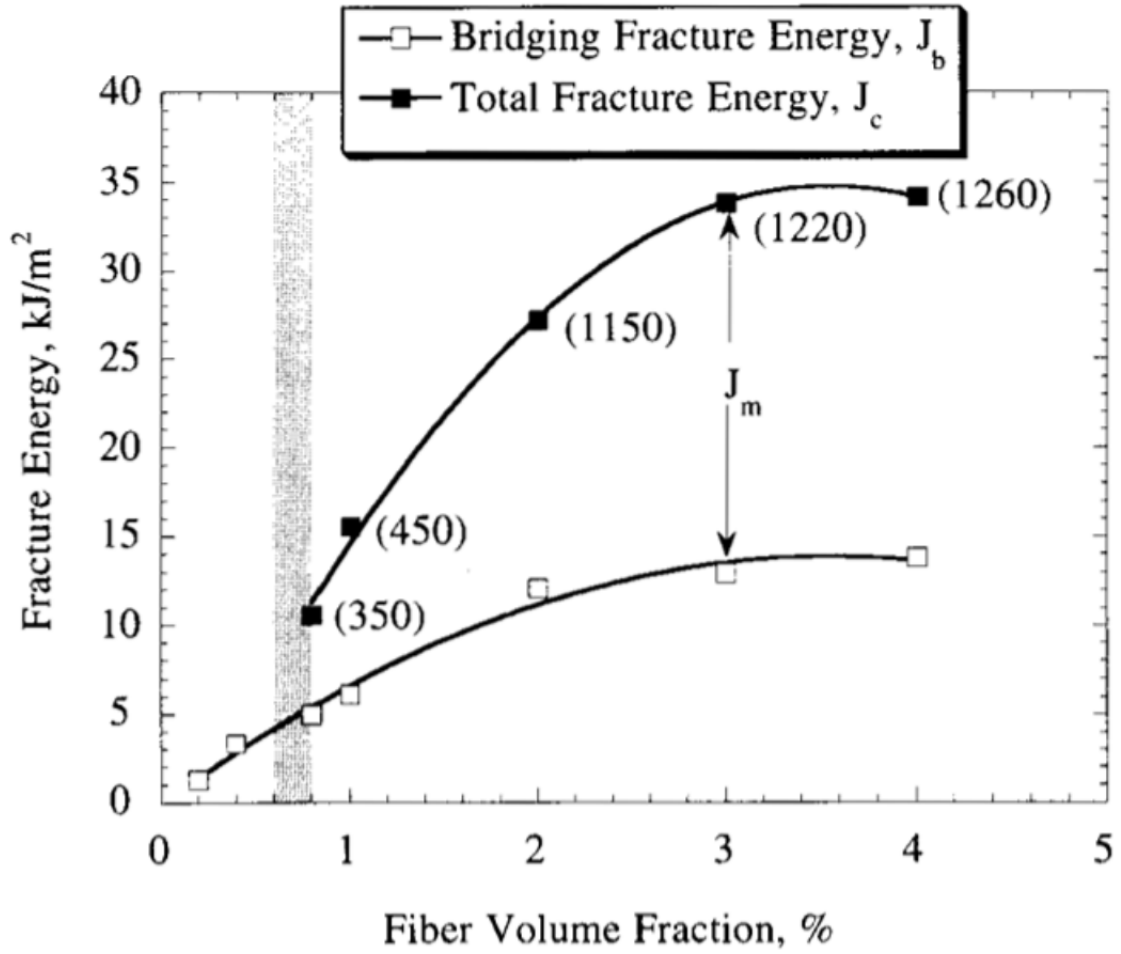


Figure 4: Fracture energy measure on and off crack plane of spectra (polyethylene) ECC. Critical fiber volume is indicated by the shaded strips [17].

2.1.4 Criteria for Strain Hardening:

In order to understand the fundamental mechanisms governing the strain-hardening behavior of ECC versus the tension-softening behavior of FRC, it was necessary to recognize and explain the load bearing and energy absorption roles of fiber bridging and multiple cracking. Now, the criteria of strain hardening will be discussed. The first criteria for strain hardening is that the matrix cracking strength including the first crack strength (σ_{fc}) associated with the first crack must not exceed the maximum bridging stress (σ_{cu}).

$$1) \sigma_{fc} < \sigma_{cu} \quad (2.5)$$

The first cracking strength can be determined experimentally and is dominated by controlling the matrix toughness and the matrix flaw size [14]. We may label this as the strength criteria for multiple cracking. This criterion is needed because prior to

flat crack (steady state crack) propagation, a micro crack must initiate from a defect site at a load level below the bridging capacity [14]. The equation used to calculate the maximum bridging stress was given before in equation (2.2).

The second criterion for strain hardening is concerned with the mode of crack propagation which in turn is governed by the energetics of crack extension. This criterion is needed for steady state cracking to occur; details leading to this criterion were discussed previously in the steady state cracking section. We may label this as the energy criterion for multiple cracking. This requires the crack tip toughness J_{tip} to be less than the complementary energy J_b' . The complementary energy J_b' was referred to as C in the figure of the previous section because the figure is old.

$$2) J_{tip} < J_b' \quad (2.6)$$

$$\text{Where } J_{tip} = \frac{K_m^2}{E_c} \quad (2.7)$$

$$\& J_b' = \sigma_0 \delta_0 - \int_0^{\delta_0} \sigma(\delta) d\delta \quad (2.8)$$

K_m = Matrix toughness & E_c = Composite Elastic Modulus

A recent σ - δ curve representing both J_{tip} and J_b' is shown below [5]. J_b' is the hatched area on the curve while J_{tip} is the shaded area. As mentioned earlier, both criteria for strain hardening are related to the fiber bridging law or the σ - δ curve which confirms its importance. The maximum bridging stress (σ_0) and the corresponding maximum opening are also shown on the figure. Moreover, the figure shows first crack or steady state stress (σ_{ss}) and its corresponding opening.

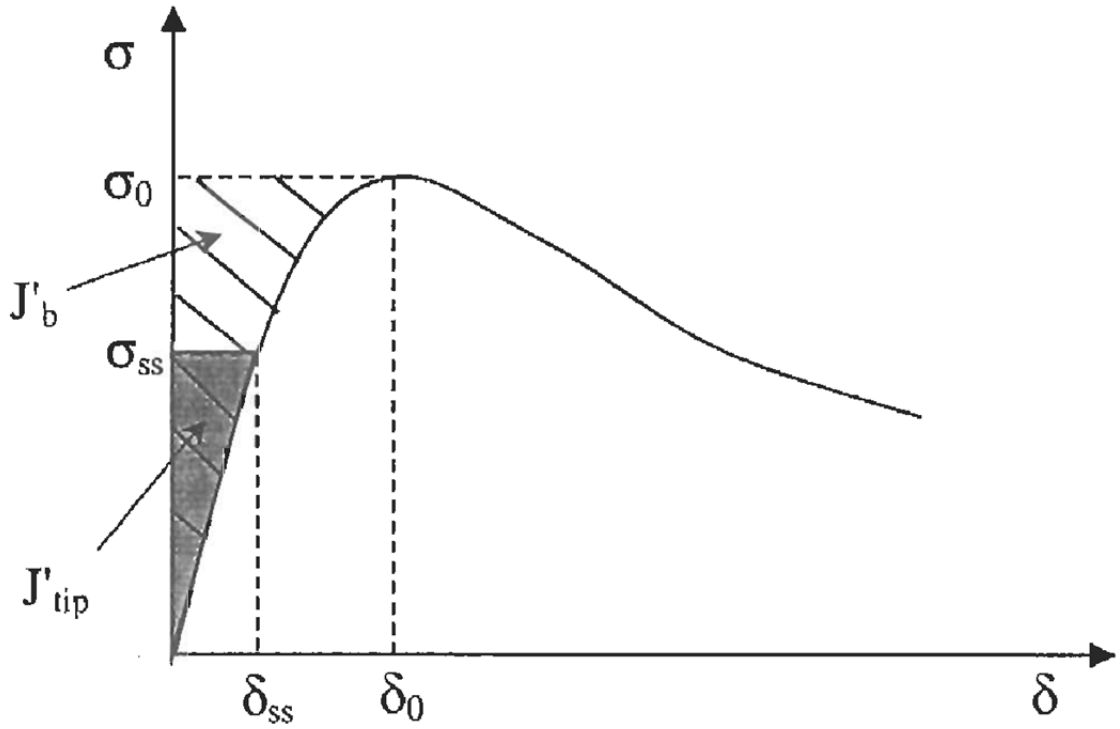


Figure 5: σ - δ curve and the concept of complementary energy (J'_b) [20].

The same criteria for strain hardening can be expressed in terms of fiber volume fraction. That is helpful because the type and quantity of fibers are key parameters influencing the performance of ECC and their cost. For instance, using a low fiber volume fraction while still attaining strain-hardening is considered very attractive from the cost point of view [3]. Also the fiber volume is really important in ECC because it affects workability, strain hardening, toughness, and load carrying capacity of the composite. To achieve pseudo strain hardening the equation for critical fiber volume is given as:

$$V_f \geq V_{fcritical} \quad (2.9)$$

$$V_{fcritical} = \frac{12J_{tip}}{g\tau(\frac{L_f}{d_f})\delta_p} \quad (2.10)$$

J_{tip} = Crack Tip Toughness (depends on the matrix toughness)

τ = Frictional Bond

L_f = Length of fiber

d_f = Diameter of fiber

δ_p = Crack opening corresponding to maximum bridging stress.

g = snubbing factor usually around 2

The snubbing coefficient is usually introduced to account for the interaction between the fiber and matrix [20]. The snubbing factor is unique for every fiber type.

The above equation expresses the condition for pseudo strain hardening in the form of a critical fiber volume fraction which must be exceeded to create a composite with high strain capacity [12]. Critical fiber volume is defined in terms of measurable micromechanical parameters involving matrix properties, fiber properties, interface properties and fiber/matrix interaction property. To create pseudo strain hardening with minimum amount of fiber, it is preferable to aim at low critical fiber volume. Therefore, low crack tip toughness (J_{tip}) and thus low matrix toughness (k_m), strong interfacial bond, high fiber aspect ratio and a large δp is required to attain pseudo strain hardening.

2.2 Micromechanics Summary:

In order to conclude micromechanics we can say that if both the energy criterion and the strength criterion are met, multiple cracking will be achieved which in turn leads to strain hardening. This is the only parameter which determines the transition from a catastrophic failure mode to a stable failure mode. A large margin between J_b' and J_{tip} is recommended due to the random nature of preexisting flaw size and fiber distribution in ECC [5] [7]. Therefore a pseudo strain hardening performance index (PSH) is used to evaluate the margin between them [20].

$$\text{PSH energy: } J_b' / J_{tip} \quad (2.11)$$

$$\text{PSH strength: } \sigma_0 / \sigma_{fc} \quad (2.12)$$

Materials with larger values of PSH indices have a better chance for the occurrence of saturated multiple cracking. Later in this paper, recommended values for both indices will be provided. Beside the two criteria, the successful design of ECC requires tailoring of the individual micromechanical parameters. The individual micromechanical parameters governing the behavior of ECC can be grouped into:

1. Fiber
2. Matrix
3. Interface (Fiber/Matrix)

The fiber is characterized in terms of the volume fraction (V_f), length (l_f), diameter (d_f), elastic modulus (E_f) and tensile strength (σ_{fu}). The matrix is characterized in terms of its fracture toughness (K_m), elastic modulus (E_m), and initial flaw size distribution (A_0). The interface is affected by the interfacial frictional stress (τ), the chemical bond (G_d), the snubbing coefficient (f), and the slip hardening coefficient (β). The theory is summarized in the figure below where micromechanics are shown as a tool for microstructure tailoring. That is because desired composite performance is a function of both microstructure tailoring and processing conditions. Finally, it should be noted that the micromechanics based design theory assumes perfect or uniform distribution of the fibers in the cement matrix [5] [20] [21].

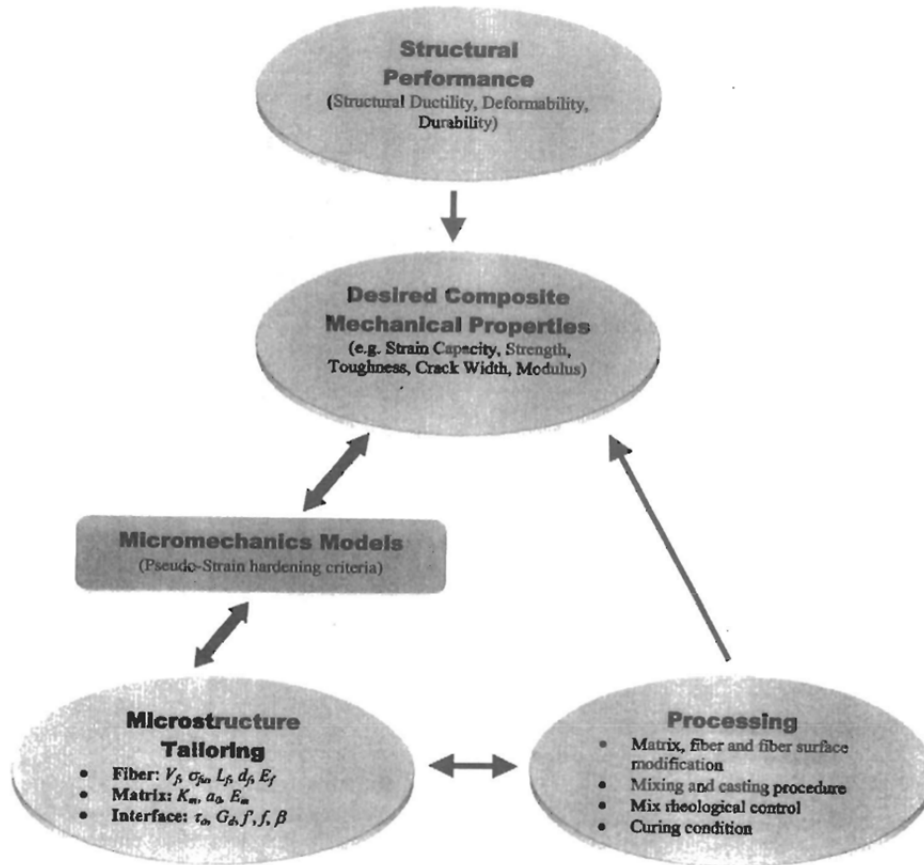


Figure 6: Micromechanics as a tool for microstructure tailoring [5].

2.3 Tailoring Individual Micromechanics Parameters:

2.3.1 Fiber:

Fibers are usually characterized in terms of volume fraction, fiber diameter and length, elastic modulus, and tensile strength [5]. These parameters influence the micromechanics results and the strain hardening behavior of ECC. As can be seen from the following equation for calculating the complementary energy (J_b'), the fiber volume (V_f), length (l_f), diameter (d_f) and elastic modulus (E_f) significantly influence the value of J_b' thus affecting the multiple cracking behavior which leads to strain hardening.

$$J_b' = \frac{V_f \tau_0^2 L_f}{6d_f^2 E_f} - \frac{2V_f G_d L_f}{d_f} + \frac{8V_f G_d}{3\tau_0} \sqrt{\frac{2E_f G_d}{d_f}} - \frac{2V_f E_f G_d^2}{\tau_0^2 L_f} \quad (2.13)$$

$$J_b' = V_f \frac{L_f}{d_f} \left(\frac{\tau_0^2 L_f^2}{6d_f E_f} - 2G_d \right) \quad (2.14)$$

The previous equations were derived from a fiber bridging law which does not account for fiber rupture, slip-hardening, and fiber orientation (snubbing factor) for simplicity [8]. To further simplify things, the last two terms of equation (2.13) were removed yielding equation (2.14). The last two terms can be removed because they have a small value [8]. As can be seen from the equation, to achieve a higher complementary energy (J_b'), a high fiber modulus and a low fiber diameter is needed. Recommended values for fiber diameters are usually between 20 to 50 microns [4]. Additionally, higher fiber length and fiber volume fraction leads to a higher (J_b'). This was also confirmed by [22]. Yet, it should be noted that excessive decrease in the fiber diameter or increase in the fiber length can lead to fiber rupture instead of pullout which is an undesirable behavior. Recommended values for fiber lengths are usually between 12 and 20 millimeters [22]. Moreover, a good fiber tensile strength is usually required in order to prevent fiber rupture so fiber bridging can occur and transfer the load back to the matrix. To ensure fibers can sustain the load, it is recommended that the fiber tensile strength is above 1000 MPa [5]. Therefore fiber tailoring is considered a major step in the design of Engineered Cementitious Composites. Experimental demonstrations of PSH indices leading to considerable strain hardening for different fiber types were obtained [20]. The following table summarizes the results collected by the study [20].

Table 2: Summary of recommended pseudo strain hardening indices.

Fiber Type:	PSH Energy	PSH Strength
Polyethylene	>3	>1.2
Polyvinyl alcohol	>3	>1.45
Polypropylene	>3	>2

Both PVA and polypropylene fibers require a higher strength index than polyethylene fibers due to their lower fiber tensile strength which translates into increased rupture tendency. This lower tensile strength also results in a larger variation of the bridging capacity [20]. Using micromechanics, (Yang & Li, 2010) [20] calculated and plotted the variation of the critical fiber volume with the frictional bond determined from both the energy and strength criterion. The following graph shows the plot for a polypropylene (PP) fiber to illustrate the concept of combining the strength and energy criteria:

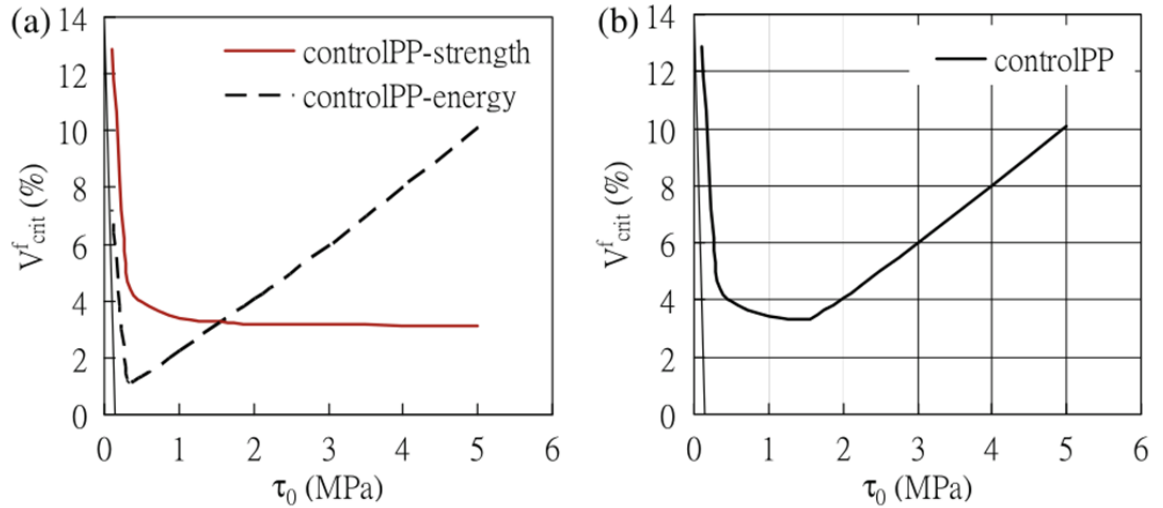


Figure 7a: Individual effects of strength criterion and energy criterion on the critical fiber volume fraction at different interfacial bond strength [20].

Figure 7b: Combined effect of energy and strength criteria on the critical volume fraction at different bond strength [20].

The graph on the right shows the combined effect of the strength criterion and the energy criterion. Another set of graphs done by the same method shows how increased fiber tensile strength reduces the critical fiber volume required for strain hardening to occur [20]. The only difference between the control PP and strong PP is the fiber strength. The tensile strength of the control PP is 400 MPa while the tensile strength of the Strong PP is 928 MPa [20].

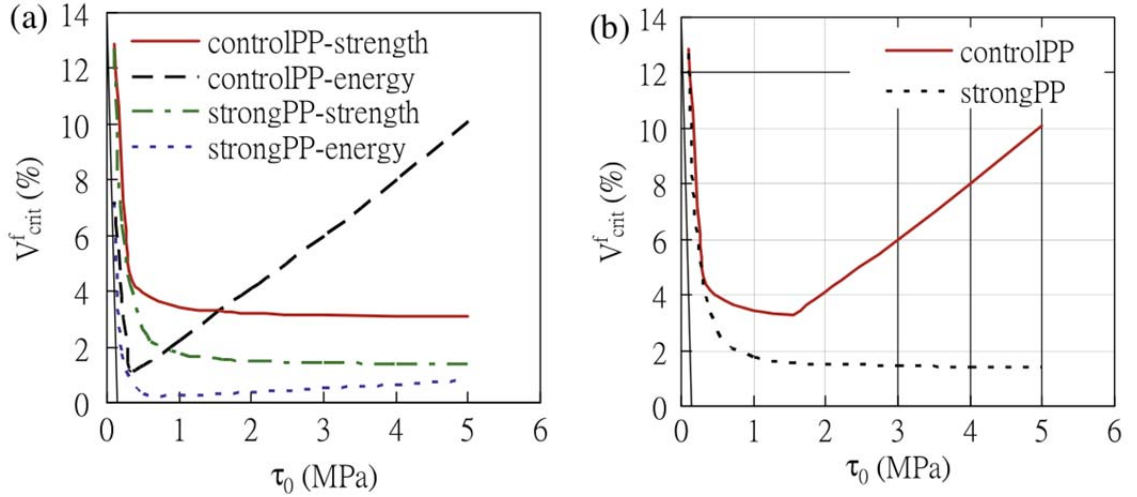


Figure 8a: Individual effects of strength criterion and energy criterion of two types of fibers on the critical fiber volume fraction at different interfacial bond strength [20].

Figure 8b: Combined effect of energy and strength criteria of two types of fibers on the critical volume fraction at different bond strength [20].

Therefore it is considered essential to tailor the fiber parameters to increase the complementary energy (J_b') and decrease the critical fiber volume (V_f) hence meeting the required PSH indices.

2.3.2 Matrix:

2.3.2.1 Matrix Toughness:

Micromechanics proved to be an effective tool that can guide the design of Engineered Cementitious composites [12]. From micromechanics formulas discussed earlier, it is clear that a decrease in the matrix toughness means higher ductility and a better strain hardening behavior [4]. The decrease in toughness is reflected by the decrease in the first cracking strength of the matrix which is usually assumed to be close to the matrix tensile strength [23]. Matrix toughness can be measured by the three point bending test described in ASTM E399 [7]. Therefore ECC typically contains two to three times more cement than conventional concrete in order to control the matrix toughness [8]. Usually between 800 and 1200 kg/m³ of cement is used [8]. The high cement content results in both a high heat of hydration and a high material cost [8]. This can be avoided by the use of High Volume Fly Ash ECC or HVFA ECC which will be discussed later in this paper. The following figure shows the variation of the frictional bond (τ) with the matrix toughness for a fixed fiber volume of 2% [23]. Mixes I, IIIa, and IIIb achieved strain hardening however Mix II

resulted in strain softening [23]. As can be seen from both the figure and the micromechanics formulas, as the frictional bond increases a higher matrix toughness can be used to achieve strain hardening behavior. Also as the bond increases a lower volume is required for strain hardening behavior.

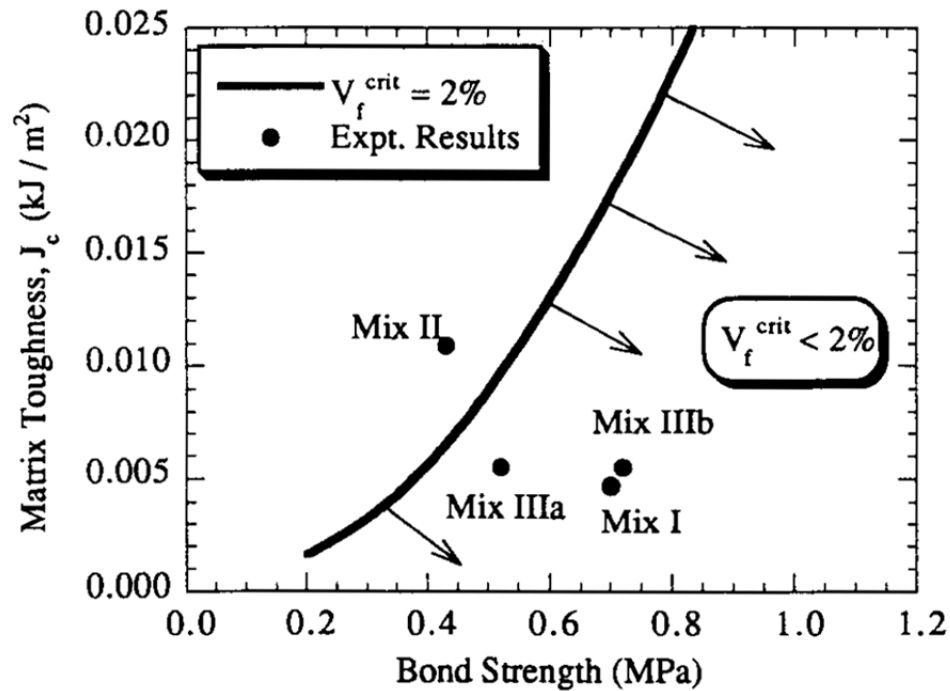


Figure 9: Variation of matrix fracture toughness with interfacial bond, strength, and critical fiber volume fraction [23].

2.3.2.2 Sand to Cement Ratio & Water to Cement Ratio:

A study [23] showed that the addition of aggregates improves the elastic modulus of ECC however excessive use of fine aggregates can suppress the pseudo strain hardening behavior. That is because the addition of aggregate raises the matrix toughness. Therefore the sand to cement ratio must be selected carefully so that it does not increase the toughness a lot. A sand to cement ratio of 0.37 was thought to be suitable for the production of good ECC [23] [24]. However later in this report, it will be shown that some aggregates like limestone can decrease the matrix toughness when added to the mix due to its very small particle size. The following graph shows the effect of sand to cement ratio and water to cement ratio on the matrix toughness [23]. As the water to cement ratio rises, the matrix toughness decreases. Also as the sand to cement ratio increases, the matrix toughness first increases then decreases nevertheless this decrease is limited. These results confirm what we learned in class

about the relationship between matrix toughness and sand to cement ratio. Furthermore, it was found that the water/cement ratio and the sand/cement ratio can slightly influence the bond strength (τ) [23].

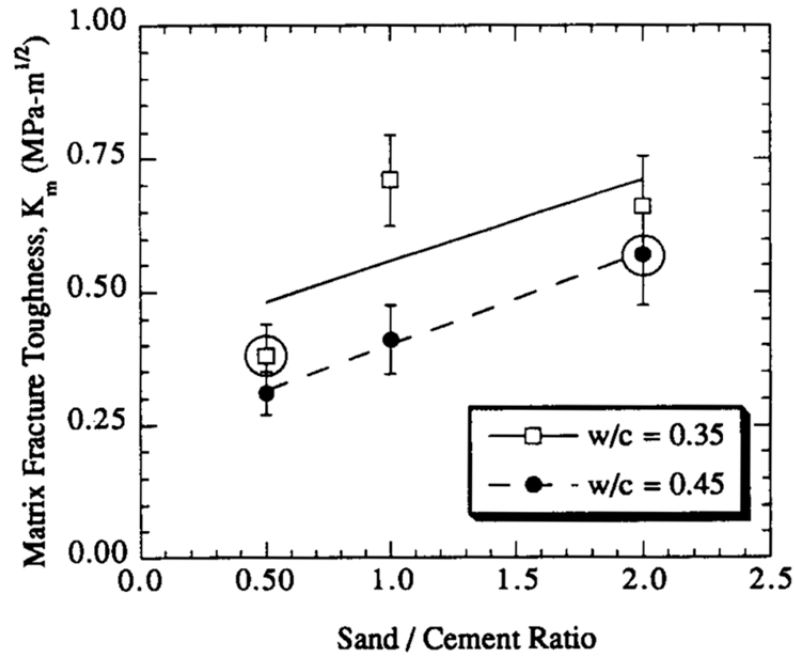


Figure 10: Matrix toughness variation with sand/cement ratio for two water/binder ratios [23].

2.3.3 Interface:

From micromechanics, it is evident that properties for pseudo strain hardening behavior are strongly influenced by fiber/matrix interface parameters. Reviewing previous micromechanics formulas such as equation 2.2, 2.10, and 2.14, which are listed below for easier access, it is obvious that an increase in frictional bond strength leads to a reduction in the fiber volume required for strain hardening. In equation 2.10, the conditions for pseudo strain hardening are expressed in the form of critical fiber volume fraction [12]. Whereas equation 2.2 calculates the maximum bridging stress corresponding to a crack opening of δ and also shows that an increase in frictional bond increases the maximum bridging stress which is preferable for pseudo strain hardening [12]. Moreover, it is evident from equation 2.14, which is the simplified micromechanics formula for calculating the complementary energy J_b' , that the chemical bond decreases the value of J_b' [8].

$$V_{fcritical} = \frac{12J_{tip}}{g\tau(\frac{L_f}{d_f})\delta_p} \quad (2.10)$$

$$\sigma_{cu} = \sigma_0 = \frac{g\tau V_f L_f}{2d_f} \quad (2.2)$$

$$J'_b = V_f \frac{L_f}{d_f} \left(\frac{\tau_0^2 L_f^2}{6d_f E_f} - 2G_d \right) \quad (2.14)$$

Therefore it is important to tailor the interfacial characteristics in the design of effective Engineered Cementitious Composites. To do this, a method for measuring the interfacial properties is required. This is usually done by fiber pullout tests. A general profile of a fiber pullout test is shown in the figure below.

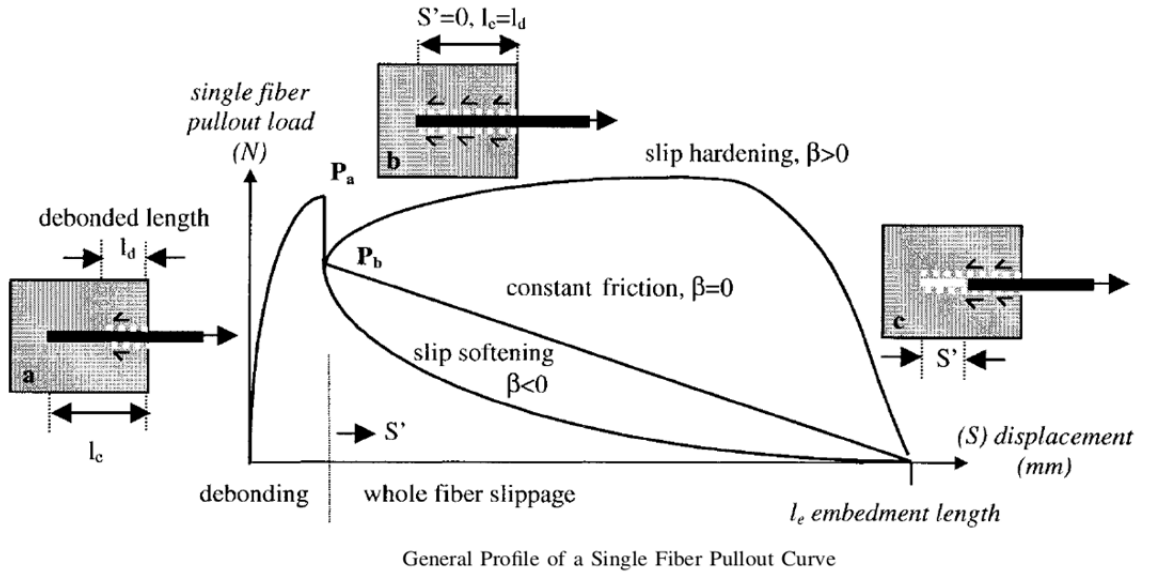


Figure 11: General fiber pullout test profile showing slip hardening, slip softening and constant friction [25].

The following equations are used to calculate (G_d), (τ), and (β):

$$G_d = \frac{2(P_a - P_b)^2}{\pi^2 E_f d_f^3} \quad (2.15)$$

$$\tau_0 = \frac{P_b}{\pi d_f l_e} \quad (2.16)$$

$$\beta = (d_f / l_f) \left[(1 / \tau_0 \pi d_f) (\Delta P / \Delta S')|_{S' \rightarrow 0} + 1 \right] \quad (2.17)$$

When friction increases during fiber slippage, slip hardening occurs [25]. This behavior can be beneficial for strain hardening and is denoted by beta (slip hardening coefficient). However, very high slip hardening can cause fiber de-lamination or

rupture [25]. According to the several researches [6] [26], there are three general types of bond strengthening mechanisms which include fiber deformation, interface densification, and fiber surface modification. Fiber deformation techniques include twisting, crimping, pitting, and button-end creation [26]. Fiber surface modification methods include chemical oxidation, corona treatment, and plasma treatment [26]. Details of these techniques and methods can be found elsewhere [26] [27]. Here the focus is given to common strengthening methods used on a variety of fiber types such as polyethylene and polypropylene. Sometimes treatment is required to decrease the bonds instead of strengthening it such as in the case of polyvinyl-alcohol fibers.

2.3.3.1 Polyethylene Fibers:

Polyethylene fibers are assumed to have no chemical bond (G_d) when incorporated in a cement matrix. This makes the focus on the frictional bond (τ) when using polyethylene as the main fiber in ECC. Typical values for the frictional bond (τ) of virgin and plasma treated polyethylene fibers calculated from equation (2.2) are listed in the following table [26].

Table 3: Typical frictional bond values of virgin and treated polyethylene fibers [26].

Plasma treatment	σ_{cu} (MPa)	τ (MPa)	Average τ (MPa)
Virgin	5.1	0.76	0.63
	4.1	0.61	
	4.2	0.63	
	3.6	0.54	
Ar	5.8	0.82	0.76
	4.7	0.70	
	4.8	0.72	
CO ₂	5.5	0.82	0.83
	5.9	0.88	
	5.2	0.78	
NH ₃	5.8	0.87	0.85
	5.5	0.82	

In the previous table, the snubbing factor (g) for polyethylene was assumed to be 2 considering it similar to polypropylene having a g value of 1.78 [26]. This assumption slightly affects the accuracy of the calculations. The value was assumed because at the time of the research there was no available measurement for the value

of the snubbing factor for polyethylene [26]. Therefore a pullout test was conducted to further verify the results of the bond strength increase [26]. The pullout results are shown in the following figure:

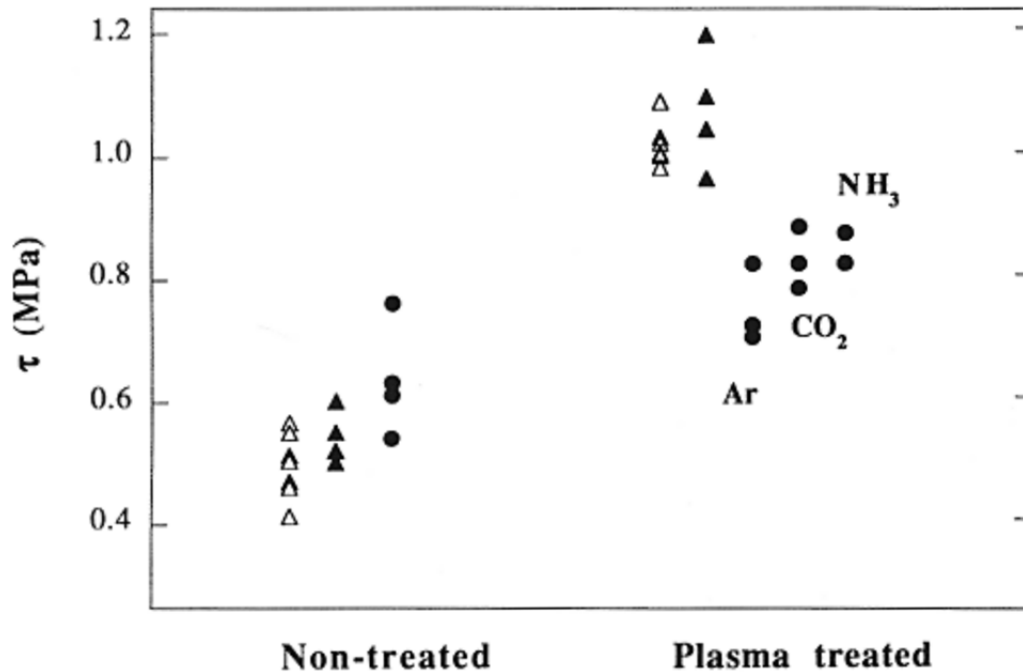


Figure 12: Effect of plasma treatment on the frictional bonds of polyethylene ECC. Triangular symbols are bond strength from pullout test. Circular symbols are bond strength deduced from composite tensile test. Open symbols indicate cement matrix without silica fume [26].

As can be seen the measured values of the bond are slightly higher than the calculated ones. However this proves the hypothesis that plasma treatment increases the frictional bond strength. Moreover, this increase in strength can be noticed from the load curve of the single fiber pullout test shown below. Following the experimental results above it can be concluded that plasma treatment is considered an effective method for strengthening polyethylene fibers.

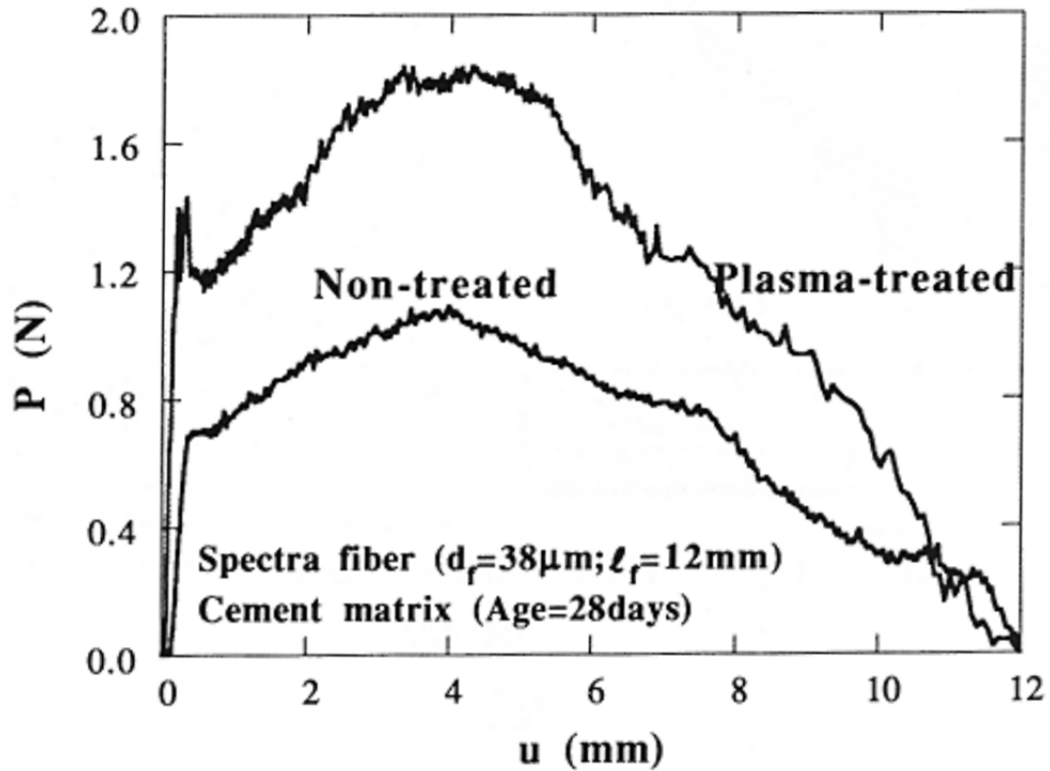


Figure 13: Pullout tests of plasma treated and non-treated polyethylene fibers [26].

2.3.3.2 Polyvinyl-alcohol Fibers:

In the past, practical applications of ECC were limited due to the high cost of the ultra-high molecular weight polyethylene fibers [6]. Attempts to use polyvinyl-alcohol fibers, which are about 8 times cheaper than polyethylene fibers, resulted in a tensile strain of 0.5 to 1% which is much lower than the tensile strain achieved by polyethylene fibers [5] [6]. The cause of this low tensile strain for a fiber having a relatively high tensile strength was identified. The reason was that PVA fibers tend to develop very strong chemical bonding with cement due to the presence of hydroxyl group in its molecular chains [6]. Also [25] showed that during PVA fiber pullout a strong slip hardening response exists which can lead to a shear delamination failure of the PVA fiber. Therefore a much greater tendency of fiber rupture is expected when PVA ECC is used without interface tailoring [6]. Single fiber pullout tests indicated typical values of the chemical bond (G_d) for PVA fibers to be in the range of 3 to 5 J/m^2 [6]. This is very high compared to polypropylene fibers which have no chemical bond (G_d) in a cement matrix [6]. It is known from micromechanics that the higher the chemical bond (G_d) the lower the complementary energy J_b' which is required for strain hardening. Moreover, as mentioned earlier when the frictional bond (τ)

increases, J_b' also increases however a very high frictional bond (τ) can lead to fiber rupture as in the case of PVA fibers. Therefore a solution was developed to decrease both the chemical and frictional bonds of the PVA fibers. Oiling of the fibers decreased the frictional bond, chemical bond, and the slip hardening coefficient and made PVA fibers achieve 5 times higher strain in ECC [6]. In another study [15] optimal ranges of the chemical bond, frictional bond, and slip hardening coefficient for the PVA fiber were established. Those ranges are $G_d < 2.2 \text{ J/m}^2$, τ between (1.0 and 2.1 MPa) and $\beta < 1.5$. The following table shows the effect of oiling quantity on τ , G_d , and β . Furthermore, the next table shows the effect of the oiling agent on the experimentally measured tensile properties of ECC.

Table 4: Effect of fiber oiling on the interfacial properties and complementary energy of ECC [6].

Oiling quantity, %	τ_0 , MPa	G_d , J/m ²	β	J_b' , J/m ²	J_b'/J_{tip}
0.0	2.44 ± 0.49	4.71 ± 0.58	2.21 ± 0.71	$3.64 - 6.63$	$0.73 - 1.33$
0.3	2.15 ± 0.19	3.16 ± 0.66	2.31 ± 0.19	$5.17 - 13.8$	$1.03 - 2.76$
0.5	2.14 ± 0.15	2.96 ± 0.75	1.82 ± 0.23	$7.68 - 13.6$	$1.54 - 2.72$
0.8	1.98 ± 0.13	2.18 ± 0.39	1.18 ± 0.34	$12.5 - 20.7$	$2.50 - 4.14$
1.2	1.11 ± 0.13	1.61 ± 0.60	1.15 ± 0.17	$24.2 - 38.1$	$4.84 - 7.62$

* $J_{tip} \sim 5 \text{ J/m}^2$ assumed for J_b'/J_{tip} calculations.

Table 5: Effect of oiling agent on experimentally measured mechanical properties of ECC [6].

Oiling quantity, %	First crack strength σ_{fc} , MPa	First tensile strength σ_{cu} , MPa	Strain capacity ϵ_{cu} , %	Crack opening x_d , mm	Crack opening, μm
0.0	3.11 ± 0.23	4.89 ± 0.07	0.99 ± 0.57	27.00 ± 12.00	43 ± 20
0.3	2.63 ± 0.43	4.72 ± 0.17	1.55 ± 0.33	7.50 ± 2.80	44 ± 7
0.5	2.35 ± 0.21	4.09 ± 0.22	2.73 ± 0.78	3.50 ± 1.10	52 ± 10
0.8	2.90 ± 0.10	4.62 ± 0.36	3.81 ± 1.14	2.50 ± 0.33	71 ± 9
1.2	2.92 ± 0.06	4.41 ± 0.15	4.88 ± 0.59	2.80 ± 0.52	88 ± 12

It is clear how tailoring the fiber/matrix interface improved the tensile strain capacity from 1% to approximately 5%. However this is not the only method for tailoring the interface properties of PVA ECC, later in this report studies showing the influence of fly ash on the interfacial bonds will be presented.

2.3.3.3 Polypropylene Fibers:

Like polyethylene fibers, polypropylene fibers are assumed to have zero chemical bond with the cement matrix. This makes the focus on the frictional bond (τ) when using polypropylene as the main fiber in ECC. The following pullout load test compares the behavior of plasma treated and untreated polypropylene fibers [27]. As can be seen from the figure, the value of the frictional bond improved slightly however the slip hardening behavior improved significantly. It was found that the frictional bond of treated polypropylene fibers improved by 20% over untreated polypropylene fibers [27].

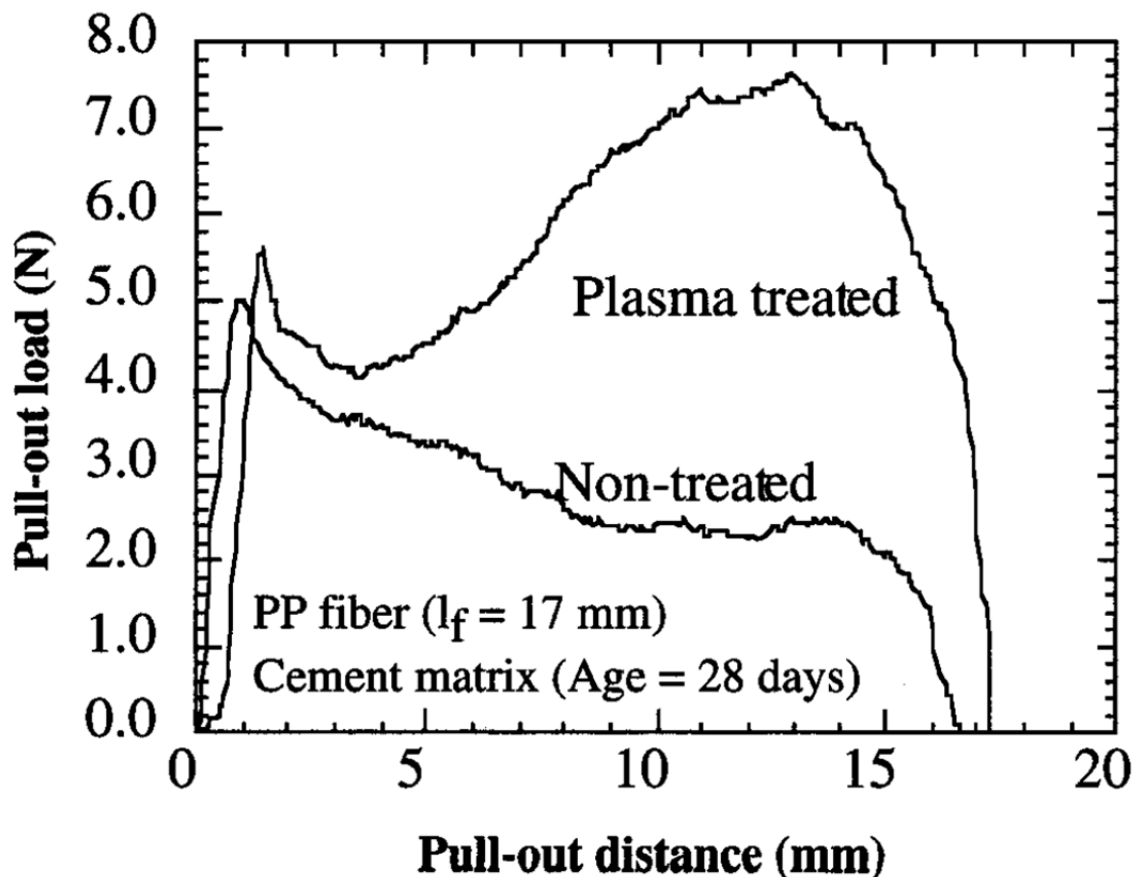


Figure 14: Pullout tests of plasma treated and non-treated polypropylene fibers [27].

2.4 Effect of Aggregates on ECC:

In normal Portland cement concrete, coarse aggregates are considered a major contributor to strength and dimensional stability of the concrete. However, Engineered Cement Composites are usually produced without adding coarse aggregates. In ECC, the fibers can act as coarse aggregates resisting a portion of the compression and tension loads. Apart from the positive contributions of coarse aggregates to concrete, the lack of coarse aggregates can have many benefits in fiber reinforced concrete especially in strain hardening cement composites. For instance, the lack of coarse aggregates increases the workability of the composite. Also, when fibers are present with coarse aggregates having a size larger than the average fiber spacing, balling of the fibers occurs [24]. Due to the effect of balling, the increase in aggregate particle size makes it difficult to spread the fibers uniformly in the mixture [24]. Nevertheless, the main reason for not including coarse aggregates is to lower the matrix toughness so the fibers can work and achieve steady state cracking which leads to strain hardening [24]. Therefore standard ECC usually contains fine silica sand however a study [24] showed that ECC can be successfully produced with crushed sand and gravel having a higher nominal aggregate size.

Table 6: Typical size distribution of silica sand [7].

< 150 μm (0.0059 in.), %	< 100 μm (0.0039 in.), %	< 75 μm (0.0030 in.), %	< 53 μm (0.0021 in.), %
93	77	33	8

ECC produced with crushed sand or gravel maintained similar mechanical properties as standard ECC. Also, [24] investigated the effect of varying the maximum aggregate size of various sands on ECC and found that for a MAS between 1.19 to 2.38 mm there was no significant change in the compressive strength, ductility, and crack width of ECC. This led to a conclusion that increasing the maximum aggregate size will have a tiny effect on ductility, compressive strength and crack width of ECC. Furthermore in a study by [28], limestone with a mean particle size of 13.4 micro meters was successfully used to replace silica sand in ECC. The limestone ECC maintained similar mechanical properties as standard ECC such as strain hardening and multiple-cracking. The tensile and compressive strength of the matrix were negatively affected by adding limestone [28]. The reason for the decrease in strength

is due to limestone being considered as an inert filler material since only a small amount of it reacts with cement [28]. Another impact of adding limestone was a decrease in both matrix toughness and loaded crack width which are considered desirable [28]. The decrease in toughness is due to the small particle size of limestone while the decrease in crack width is due to the better packing of particles at the fiber matrix interface which is caused by the small particle size of limestone [28]. However, adding too much limestone to the matrix results in a weak fiber-matrix interface [13]. This further confirms the prediction of previous researches which recommended limiting the sand to cement ratio in ECC matrix design.

2.5 Rheological Control of ECC:

In ECC, the viscosity of the fresh mortar plays an important role in fiber distribution and is not only considered a segregation concern [29]. In a research by [29] 4 different factors affecting the rheological properties of ECC were studied. The factors include fly ash variability, high range water reducer dosage, water/binder ratio, and viscosity modification agent dosage. Results show that the water-binder ratio is the main factor controlling plastic viscosity and the HRWR is the most significant factor affecting the relative yield stress [29]. Relative yield stress and plastic viscosity are two very important rheological properties which can be directly linked to tests like mini slump test, marsh cone flow test, and funnel tests [29]. Moreover, the study concluded that ECC with adequate viscosity and good workability can be obtained by controlling the Water/Binder ratio and the HRWR/Binder ratio without the need for a VMA [29]. The main reason for avoiding the viscosity modification agent is due to its high cost. Furthermore, [29] suggested the use of saturation points for high range water reducer dosage. A previous study by [30] suggested the use of a water-binder ratio of 0.25 ± 0.05 to produce adequate ECC. Besides that, it should be noted that fiber type and length can significantly impact the workability of ECC and viscosity needed for the distribution of the fibers.

2.6 Effect of Fly Ash on ECC:

High cement content in regular ECC mixtures permit high percentage of potential cement substitution by relatively low quality fly ash without any significant compromise to strength development [8]. In a study conducted by [7], it was found that increasing fly ash proportion in an ECC matrix reduces the compressive strength

but provides many benefits which surpass the reduction in compressive strength. These benefits include tighter crack width, reduced fiber/matrix chemical bond (G_d), reduced drying shrinkage, and a reduced variability of tensile ductility [7]. Besides that, fly ash is considered a waste material and its usage in ECC improves the material greenness and promotes increased sustainability. One of the reasons for the loss of compressive strength is due to the limited secondary hydration of fly ash in HVFA ECC. Secondary hydration of fly ash is limited in HVFA ECC due to high content of fly ash which causes fly ash to remain in the system as filler material [7]. Another reason is the low water to binder ratio which confines the amount of water needed for secondary hydration [7]. Moreover, it was found that drying shrinkage decreased by 50% when FA/C ratio increased from 1.2 to 5.6 due to matrix densification effect which prevents moisture evaporation and also due to unhydrated fly ash particles serving as fine aggregates [7]. Another study by [8] investigated the effect of adding fly ash on the micromechanics of ECC and concluded that fly ash reduces the matrix toughness (K_m) and fiber/matrix chemical bond (G_d). That is because the matrix fracture energy J_{tip} as well as the matrix fracture toughness decreased when the ratio of fly ash to cement increased [8]. Furthermore, [7] showed that an increase in fly ash to cement ratio increases the frictional bond (τ) between the fiber and the matrix. However the slip hardening coefficient (β) showed little dependence on fly ash content. The effects of different proportions of fly ash on the chemical bond, frictional bond, and slip hardening coefficient are displayed in the following figures:

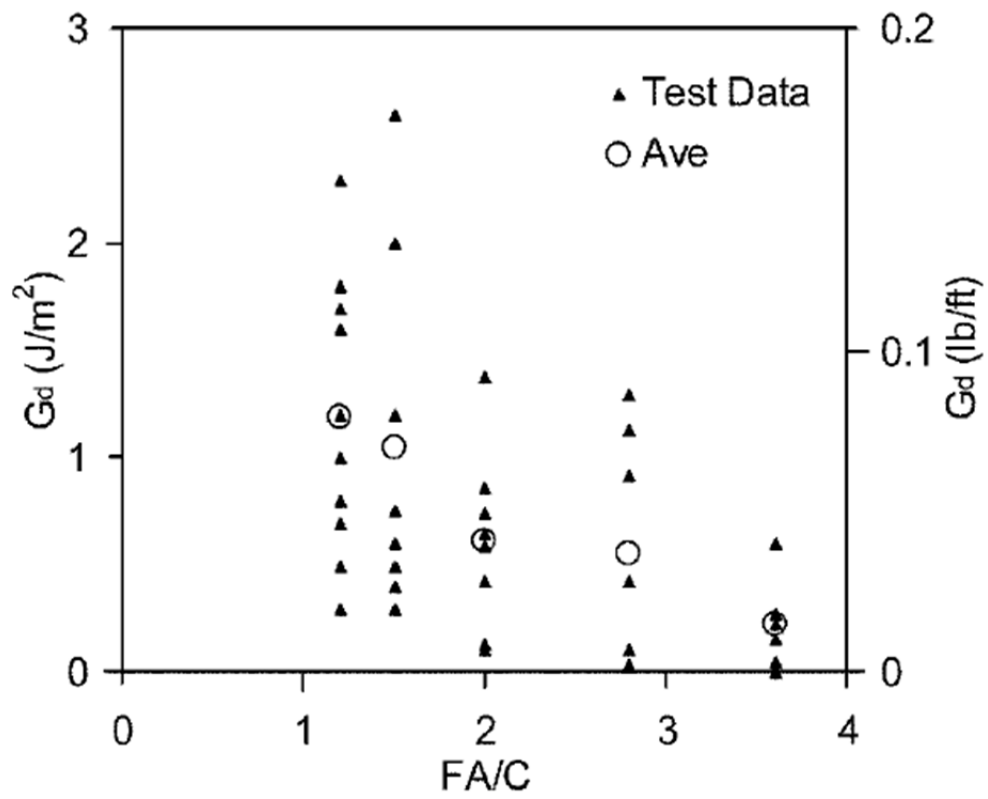


Figure 15: Chemical bond variation with increasing fly ash content [7].

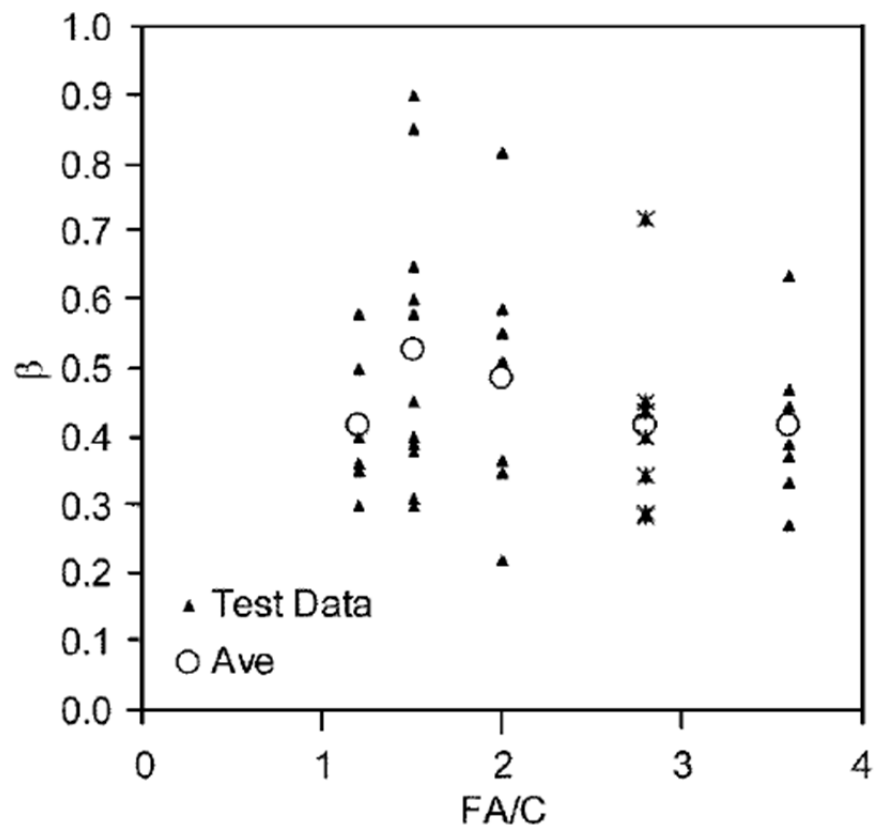


Figure 16: Slip hardening coefficient variation with increasing fly ash content [7].

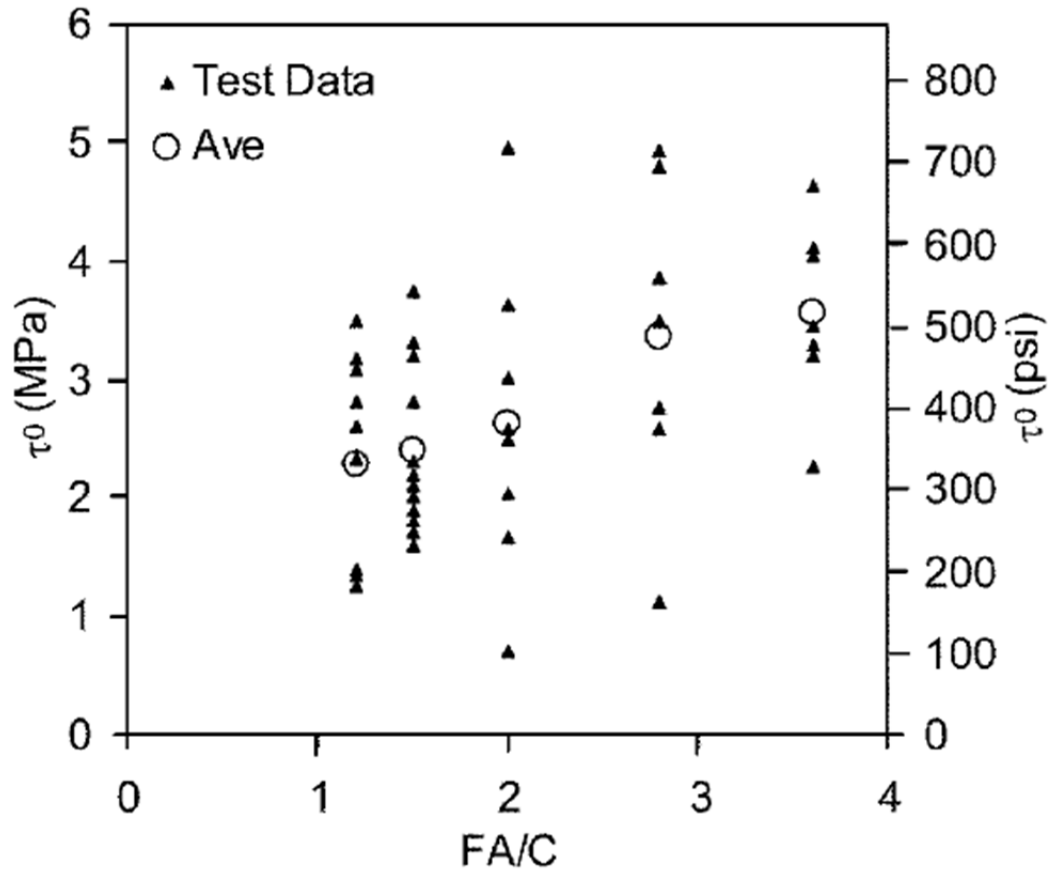


Figure 17: Frictional bond variation with increasing fly ash content [7].

In the same study by [8], another set of experiments with different types of ashes concluded that ash type shows significant effect on strength development. For instance bottom ash gained strength slower than class F fly ash. Results from other researchers concluded that as the ratio of fly ash to cement increases the strain capacity of ECC increases but the tensile strength was significantly reduced [24]. Also the same study confirms the results of the previous study which concluded that fly ash reduces the crack width [24]. Furthermore, the addition of fly ash tends to reduce the HRWR demand [24].

2.7 Effect of Blast Furnace Slag on ECC:

In a study by [31], the influence of adding ground granulated blast furnace slag on the micromechanics and the performance of ECC was evaluated. Slag was found to increase the matrix toughness and thus decrease the value of J_{tip} resulting in a decreased potential for saturated multiple cracking to occur [31]. However, slag results in better fiber dispersion due to its positive effects on the workability of fresh ECC [31]. Although it was expected that slag will decrease the strain of ECC, better

fiber dispersion led to an increase of 50% in strain [31]. It should be noted that this improvement on strain is limited to a high water-binder ratio. When a low water-binder ratio was used the effects on multiple cracking and strain hardening can be much worse. Therefore, according to [31], within a limited slag dosage the improvement on workability and fiber dispersion outweighs the decreased potential for multiple cracking. Moreover, slag was found to slightly increase the frictional bond (τ) between the fiber and the matrix [31]. However, no significant difference in the chemical bond (G_d) was observed [31]. Finally, the study suggested an optimal range of water-binder ratio (0.38 to 0.48) to be used in the production of Blast Furnace Slag ECC [31]. Furthermore, results from other studies by [28] confirmed the need for a high water to binder ratio relating it to the higher water demand of BFS compared to fly ash.

2.8 Effect of Silica Fume on ECC:

The effects of silica fume on the frictional bond strength of several fibers were summarized by [32]. The following table shows the effect of silica fume on the frictional bond [32].

Table 7: Effect of silica fume addition to ECC matrix on the interfacial frictional bond [32].

fiber	fiber modulus GPa	fiber diameter, μm	matrix composition	τ_{ave} MPa	reference
polyethylene (spectra)	120	42	w/c=0.50 SF= 0, 20%	0.40, 0.63	[36]
			w/c=0.35 SF= 0, 20%	0.56, 0.61	
carbon (smooth)	240	10	w/c=0.50 SF= 0, 20%	0.52, 0.66	[36]
			w/c=0.35 SF= 0, 20%	0.80, 1.29	
carbon (rough)	175	42	w/c=0.50 SF= 0, 20%	0.52, >2.44	[36]
			w/c=0.35 SF= 0, 20%	0.39, >3.02	
steel (rough)	210	60x120	w/c=0.35 SF= 10%	3.60- 3.98	[17]
			w/c=0.35 SF= 20%	3.73- 4.38	

It was shown that silica fume has the ability to increase the frictional bond of rough fibers by a factor between 5 to 10 [32]. This is a huge increase in the frictional bond which leads to fiber rupture. However for smooth fibers silica fume increases the bond by a factor close to 2 which is considered desirable. Nevertheless, enhancing the frictional bond by changing the matrix composition is considered less effective than using surface treatment or fiber deformation techniques [32]. Still silica fume has other effects on concrete and cement pastes including higher compressive strength and better durability.

Chapter 3: Experimental Program & Materials Characterization

3.1 Experimental Program:

3.1.1 ECC Mixture design:

The experimental program was designed after the knowledge received from the extensive literature review. The literature review aided in understanding the micromechanics based design concepts of ECC. The first goal of this research requires the use of materials available in the UAE, therefore the research focused on materials widely available in this country. Two materials widely available in the UAE are crushed limestone and dune sand. They were chosen as the basic aggregates for creating a non-standard ECC because standard ECC is made with silica sand only. Moreover, in standard ECC, an aggregate to binder ratio of 0.36 is usually used. This research uses an aggregate to binder ratio of 0.8 in order to reduce the cement volume in ECC which in turn reduces the cost. After that, several tests were done to quantify and better understand the characteristics of the materials. These tests were meant to find out numbers that can aid in the matrix design such as the particle size distribution and the specific gravity of the aggregates. Micromechanics principles were used as guidelines to design a non-standard ECC mixture that can take aggregates instead of sand. Also, the non-standard ECC mixture can take twice as much aggregate to binder ratio (0.8) as in standard ECC (0.36). Furthermore, in order to fulfill the micromechanics requirements, a rarely used technique which requires a mortar flow table was primarily used to enhance the particle packing of the matrix. This is expected to increase the fiber/matrix frictional interfacial bond so a larger amount of aggregates can be accommodated in ECC. The fiber used was a high modulus polyethylene fiber. The reason for using polyethylene fibers is due to the fact that these fibers are used in standard ECC and are considered the best for making ECC. Another reason for using these fibers is to make comparison possible with previous ECC research and to avoid interference of a new fiber type with the results. In addition, some mixtures were designed to investigate the effect of UFFA on the fresh and hardened properties of ECC. Fly ash is a mineral admixture which is known to enhance standard and non-standard ECC mixes. Basically, fly ash enhances the frictional bond of ECC and the workability of fresh ECC. Therefore, ultra-fine fly ash, which is a grinded version of fly ash that usually enhances the workability more than normal fly ash, was used. Also UFFA should be able to increase the fiber / matrix

bond and the strength of the mixture more than normal fly ash. Based on these requirements, a set of mixes were designed. The local materials which are crushed limestone and dune sand were used in all mixtures so that their suitability for making ECC can be investigated. The water to binder ratio used on the first couple of mixes was fixed at 0.3. This number was chosen to be a point of balance between matrix toughness requirements and rheological requirements for creating good ECC. Then, four mixes were added to investigate the effect of increasing the UFFA content in ECC. After that, the water to binder ratio was raised to 0.35 to see if a decrease in matrix toughness will enhance the mechanical performance of ECC. The following table shows all the mix designs used in this research:

Table 8: Mix designs

Mix#	Cement (kg/m ³)	Crushed Limestone (kg/m ³)	Dune Sand (kg/m ³)	UFFA	w/b	Water (kg/m ³)	Fiber (%)
0.3 ECC	1033	473	387	0	0.3	310	2
UFFA 10	915.95	466.46	381.64	101.27	0.3	305.32	2
UFFA 20	802.52	459.77	376.18	200.62	0.3	300.94	2
UFFA 30	692.28	453.28	370.87	296.69	0.3	296.69	2
UFFA 50	480.91	440.83	360.68	480.91	0.3	288.54	2
0.35 ECC	980.54	449.36	367.66	0	0.35	343.14	2
0.35 UFFA 50	457.97	419.80	343.47	457.97	0.35	320.58	2

As can be seen from the above table, the ECC mixtures were labeled such that the ingredients and the water / binder ratio can be identified from their name.

3.1.2 Mixing procedure and curing:

A new mixing procedure which helps in achieving better fiber distribution was used for all mixes. The new mixing procedure requires part of the water (w/b of 2.7) to be mixed with solid materials and super plasticizer for 3 minutes [33]. Then fibers are added and mixing continues for another 2 minutes [33]. After that the rest of the water is added and mixing continues for a final 2 minutes [33]. By separating the water into two parts, the plastic viscosity of the mixture increases and better fiber dispersion is achieved. Further details of the improved mixing sequence can be found in [33]. It should be noted that the fibers were dispersed by air pressure before being added to the matrix. A special tank for the dispersion of the fibers was manufactured

in the manufacturing lab at the American University of Sharjah. A picture of the tank is shown below:



Figure 18: Fiber dispersion tank.

When the mixing finished, samples were cast into molds and then cured well for 1 day using nylon sheets covered with wet burlaps. When the samples became 1 day old, they were moved into curing tanks filled with water. Proper curing of the samples was considered essential so that the mixing water does not evaporate and hence ensuring good results.

3.1.3 Uniaxial Tensile Tests & Compressive Tests:

Three samples were prepared from each mixture. The samples were tested in uniaxial tension. The dimensions of the uniaxial tensile test samples are “300 x 50 x 12 mm”. Two test parameters were generated from the tension testing. The first parameter is the load which is usually reported in Newton’s (N). This parameter will be converted to Tensile Stress by dividing it with the cross sectional area of the samples. The value of the Tensile Stress will be reported in Mega-Pascal’s (MPa). The second test parameter is the tensile extension which was reported in millimeters by the testing machine. Tensile extension can be converted to Tensile Strain by dividing it with the length of the sample that was under strain and multiplying it by 100. Strain is usually reported in percent (%). Aluminum plates were attached to the samples in order to prevent the machine from crushing the samples and to distribute stresses uniformly for the tension test. Furthermore, to get an accurate measurement of tensile strain, a fixture or stand was manufactured in the manufacturing lab at the American University of Sharjah. The fixture was used to hold two LVDT’s, which reported the exact strain capacity of the samples. This procedure was applied in order to avoid any slippage that can be caused by the aluminum plates which were attached to the samples. The following figure shows the tension test:

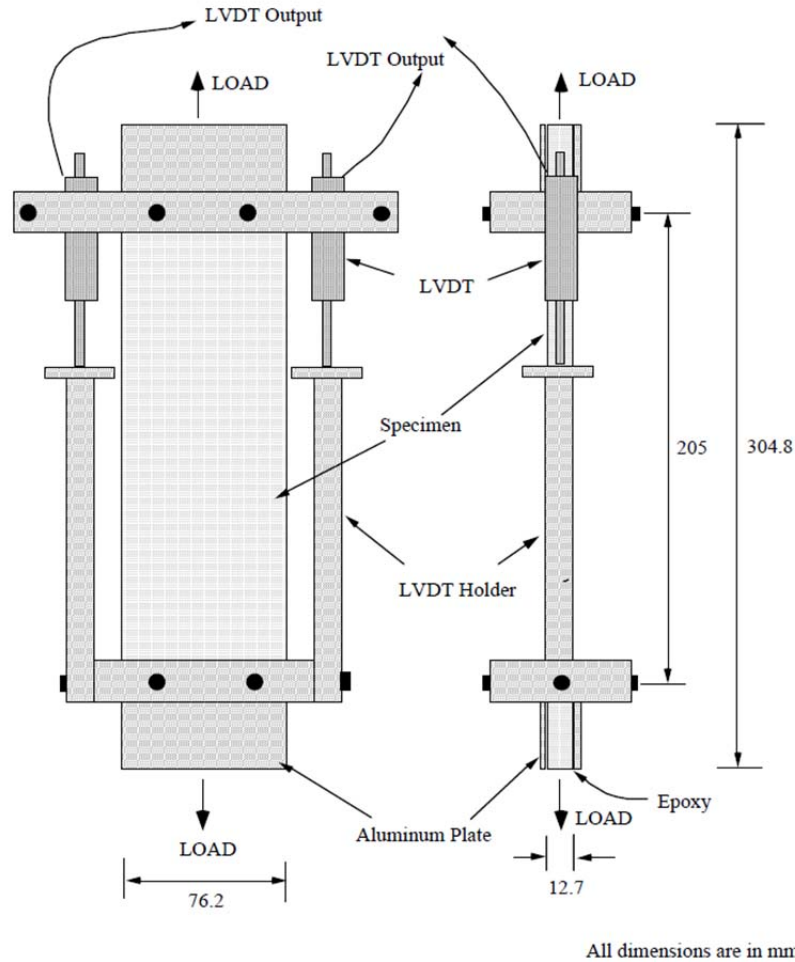


Figure 19: Tensile test layout [2].

Furthermore, compressive tests were done on cubes containing mortar to determine the compressive strength of the ECC mixtures. Also another compressive test was done on an ECC mixture which consists of the same mortar but includes fibers. The dimensions of the cubes which were used for the compressive strength tests are “50x50x50 mm”. Compressive tests were done on both 7 and 28 days. In the end, when the data became available, several graphs and figures were generated to properly analyze the data and draw useful conclusions.

3.2 Materials Characterization:

3.2.1 Aggregates:

The first goal of this research is to produce ECC using local materials available in the UAE. Standard ECC is made using very fine silica sand instead of aggregates in order to reduce the matrix toughness of the mix. However several researchers succeeded in producing ECC with fine aggregates. The use of aggregates

reduces the water demand of the mix since the surface area of the aggregates is less than the surface area of the sand particles. Also aggregates can increase the compressive strength of the matrix and reduce the cost of producing ECC. Researchers who used aggregates in ECC theorize that the increase in toughness due to the increase in aggregate size and amount can be offset by adding mineral admixtures such as fly ash [34] [24]. Two of the most important factors in designing any matrix are the quality and choice of materials. Therefore in order to distinguish between materials, several tests should be conducted on them. The following are tests typically done on aggregates.

- a. Sieve Analysis
- b. Specific Gravity & Absorption
- c. Moisture Content
- d. Chemical Composition

Two of the most available aggregates in the UAE are limestone and dune sand. Since dune sand is very similar in particle size to silica sand, it was chosen to be used in this research. The following table shows a comparison between the particle size distribution of dune sand and silica sand.

Table 9: Particle size distribution of silica sand and dune sand.

Sieve Size:	600 μm	300 μm	150 μm	100 μm	75 μm	53 μm
Silica Sand	-	100	93	77	33	8
Dune Sand	99.8	98	50.9	-	4.5	-

The particle size distribution of dune sand shown above was obtained from a sieve analysis conducted in the soil lab of the American University of Sharjah. However, the silica sand particle distribution data was obtained from a published research on ECC [7]. It is clear that dune sand particles have a size distribution between 300 and 75 microns with an average size around 150 microns. While silica sand has a particle size distribution between 150 and 53 microns with an average size around 90 microns. Even though dune sand is a little coarser than silica sand, both sands belong to the same category and can be classified as silts. Since ECC uses only one type of sand as its aggregate component, the grading in most standard ECC is poor. Therefore, this research sought to enhance the grading and in turn the particle packing of the matrix by adding another type of aggregate having a different particle size distribution. The second type of aggregate was chosen to be crushed limestone

since it is abundant in the UAE. Its chemical composition was found to be 97.5% CaCO_3 . A sieve analysis was conducted to find the particle size distribution of crushed limestone. The results are shown below:

Table 10: Particle size distribution of crushed limestone.

Sieve Size:	2.36 mm	1.7 mm	1.18 mm	600 μm	300 μm	150 μm	75 μm
Crushed Limestone	100	98	62.1	8.2	1.9	1.7	1.6

Most crushed limestone particles are distributed between 1.7 mm and 300 microns. Therefore combining dune sand and crushed limestone should give a much better aggregate grading than the one found in standard ECC. Some might argue that the maximum particle size of crushed limestone (1.73 mm) is much higher than silica sand which will eventually lead to high matrix toughness. That is true however researchers were able to make ECC with different types of crushed sand having a maximum particle size of 2.38 mm [24]. Yet this reduced the strain capacity of ECC from 5% to 2% but a 1% regain in strain was achieved by adding mineral admixtures such as fly ash [34] [24].

In order to design a matrix which includes two types of aggregates, the specific gravity and absorption of aggregates are needed. Also, the moisture content of the aggregates is required for water corrections. Therefore, specific gravity and absorption tests and moisture content tests were conducted on both crushed limestone and dune sand. The results are shown below:

Table 11: Specific gravity, absorption, and moisture content test results for the local materials.

Aggregate type:	Crushed Limestone	Dune Sand
Specific Gravity (Oven Dry)	2.661	2.605
Specific Gravity (SSD)	2.678	2.635
Apparent Specific Gravity	2.710	2.685
Absorption (%)	0.65	1.14
Moisture Content (%)	0.076	0.414

The next step is to determine the proportion of each aggregate type to be used in the mix design. A useful technique that is rarely used was implemented to determine the optimum ratio of aggregates. The technique requires a mortar flow table and is based on the idea of determining the proportion of aggregates which provides the highest mortar spread on the flow table. The highest flow or spread value translates to the best workability and highest particle packing. Researchers [35],

proved that better workability means better particle packing. Also some researchers [35], used the same technique to make a very high strength (150 to 200 MPa) concrete. Mortar flow tests adhering to ASTM Specification C1437 were conducted and that is by using an automatic mortar flow table corresponding to ASTM specifications C230 / C230M. The mortar flow tests were conducted on eight different mixes. In those mixes, the aggregate to binder ratio and the water to binder ratio were held constant. The only thing varying is the proportion of both aggregates (dune sand and crushed limestone). The mortar was mixed according to the standard practice for mechanical mixing of hydraulic cement pastes and mortars of plastic consistency (ASTM C305). Values of the water to binder ratio (0.485) and the aggregate to binder ratio (2.75) were chosen from the standard mix to be used with the mortar flow table which can be found in ASTM C109. The following table shows the results of the flow tests:

Table 12: Mortar flow test results of varying aggregate ratios.

Dune Sand Content (%)	Average Flow Diameter (cm)
0	14.662
20	16.655
30	17.678
40	18.005
45	18.552
50	17.262

The first mix contains only crushed limestone. As more dune sand is added to replace the crushed limestone, the average flow diameter increases until the dune sand content reaches 45%. After that the flow decreases with increasing dune sand content. The results show that at 45% dune sand content, we have the best flow which also means the best particle packing and the least friction between the aggregate particles. Based on these results, aggregate proportions of 45% dune sand and 55% crushed limestone were used for all ECC mixes.

3.2.2 Fibers

The fiber is the main component of ECC and is the major player in achieving the high strain capacity of the material. After a long search in the UAE market, it was concluded that none of the fibers available in the UAE comply with the recommended standards of making ECC which were mentioned earlier in the literature review. Therefore, the fiber was ordered from the United States. A polyethylene fiber which is

considered the best fiber available to make ECC was chosen due to its high strength and modulus. PVA fibers were not considered due to the high chemical bond they create when added to a cementations material. Also polypropylene fibers were out of consideration due to their low strength and modulus. The fiber characteristics are mentioned in the table below:

Table 13: Polyethylene fiber specifications.

Fiber Type	Ultra High Modulus Polyethylene Fiber
Tensile Strength	2500 MPa
Modulus of Elasticity	70 GPa
Fiber Length	12 mm
Fiber Diameter	38 μm
Specific Gravity	0.96

3.2.3 Cement

The chosen cement type for this research was a standard CEM TYPE I 42.5 cement. The cement origin facility is the Sharjah Cement Factory. Different types of cement can have effects on the mechanical performance of any concrete or ECC mixture. Yet changing or varying the type of cement is out of the scope of this thesis.

3.2.4 High Range Water Reducer

The high range water reducer used in this research was Glenium-110M. Glenium-110M is a high performance concrete super-plasticizer based on modified polycarboxylic ether and is a product of BASF Construction chemicals LLC. The specific gravity of this product is 1.07. Also the normal dosage of Glenium-110M is between 0.5 and 1.5 liters per 100kg of cement or cementitious materials. The cementitious materials content used to make all the non-standard ECC mixtures in this research is about 1000 kg/m^3 . This means that according to the product data sheet of Glenium-110M, the minimum HRWR dosage should be 5 liters and the maximum should be 15 liters. It will be shown later that a much lower dosage of the HRWR (3 liters and lower) was used in this research and that is due to the good workability of the mixture which was achieved by using the flow table method to enhance the particle packing of the mixture.

Chapter 4: Test Results and Discussion

4.1 Test Results:

4.1.1 Compressive Strength:

The compressive strength of mortar containing fine aggregates which is designed for ECC mixtures was tested at 7 days and 28 days. The mortar was made of crushed limestone, dune sand, cement, and water. The water / binder ratio used is 0.3 and the aggregate to binder ratio is 0.8. The test was done according to ASTM C109 using 50 mm cubes. Only one cube was tested at 7 days while two cubes were tested at 28 days. The results are shown below:

Table 14: Compressive strength results of mortar and ECC mixtures.

Test Number:	7 days (MPa)	Sample 1 28 days (MPa)	Sample 2 28 days (MPa)	Average 28 days (MPa)	Density (kg/m ³)
Test 1 (no fibers)	71	60	81	70.5	2352
Test 2 (no fibers)	57	81	83	82	2320
Test 3 (with fibers)	53	71	70	70.5	2120

Due to the large variation in the 28 days results of test 1, another test was performed and was called test 2. The mix used for test 2 is exactly similar to the mix used in test 1. However, in test 2, the molds were replaced as they were thought to be the cause of the large variation in compressive strength. Test results showed the previous assumption to be true. After that, fibers were added to the mortar to create ECC and the test was called test 3. When the fibers were added to the mortar, they created some empty spaces in the matrix next to the walls of the molds. These empty spaces reduced the density of the cube from 2320 to 2120 kg/m³. The spaces can be eliminated by vibrating the mixture on a vibrating table however that was not done for all the compressive tests in order to comply with the ASTM C109 specifications. It was noted later that in all samples prepared for tension testing, one can hardly observe a bubble or an empty space on the surface of the samples. That is because all the samples prepared for tension testing were vibrated. It can be concluded from the above test results that the addition of fibers to the mortar did not cause any significant increase in the compressive strength of the matrix. Also, the results suggest that the ECC samples have a compressive strength of about 80 MPa or higher at 28 days. Furthermore, it was found that test 3 cubes which include fibers deformed by

decreasing more than 25 mm in height which is exactly half the height of the cube while increasing in both length and width. The cube can be seen in the picture below:



Figure 20: Deformed ECC cube.

4.1.2 Tensile Strength & Tensile Strain:

The average 14 days tensile strength and tensile strain test results of the ECC mixtures incorporating different Water / Binder ratio and different Ultra-fine fly ash content are shown below:

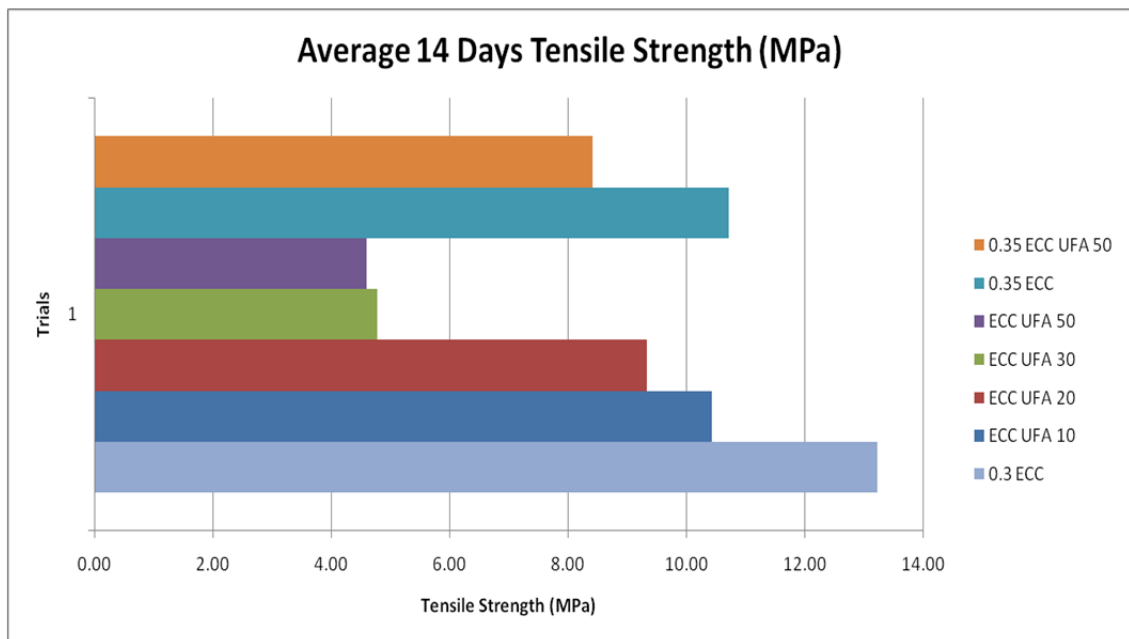


Figure 21: Average 14 days tensile strength of all the tested ECC mixtures.

As expected, the tensile strength of the ECC samples is decreasing with increasing fly ash content. This is especially true for 14 days results where the ultra-fine fly ash did not complete its hydration. Tensile strengths up to 12 MPa were achieved. However the average tensile strength of all the ECC samples produced in this research is 8.5 MPa at 14 days. This is expected to increase to 10.5 MPa at 28 days. The high tensile strength of this type of ECC was not observed in previous research. This behavior is possibly due to the high frictional bond between the polyethylene fiber and the matrix which is primarily caused by the enhanced particle packing density of the aggregates. Also, ECC with aggregates can take more tensile and compressive strength than standard ECC. The following are tensile strain test results of ECC mixtures incorporating different Water / Binder ratio and different Ultra-fine fly ash content:

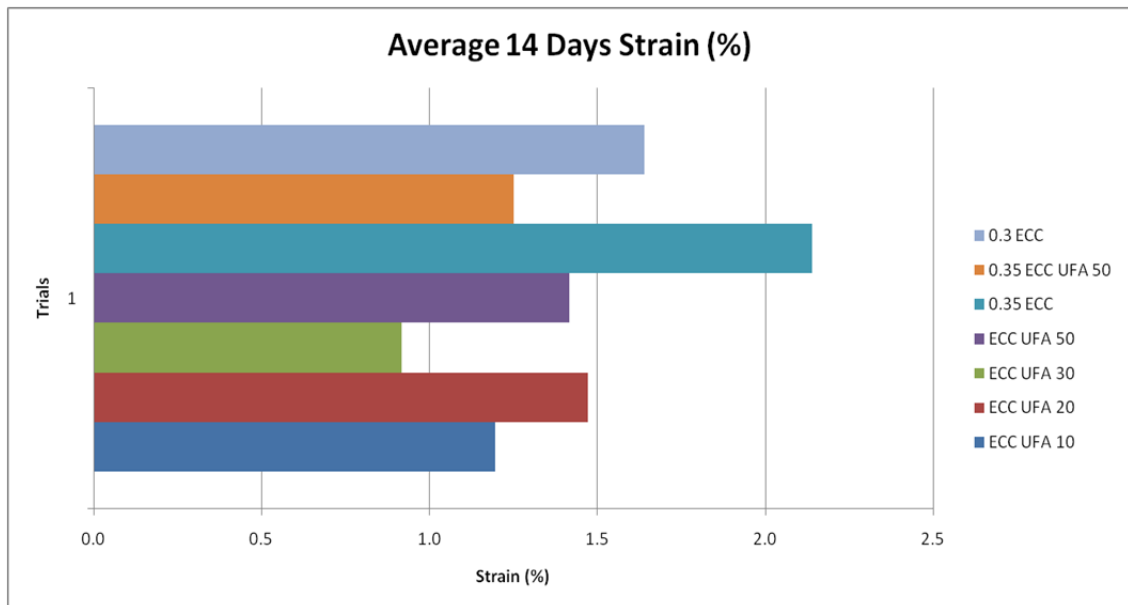


Figure 22: Average 14 days tensile strain of all the tested ECC mixtures.

ECC samples produced with a water/binder ratio of 0.3 are expected to have a higher value of the matrix toughness than ECC samples produced with a water / binder ratio of 0.35. Therefore the 0.35 samples are expected to perform better in terms of tensile strain. As can be seen from the graph, tensile strains of around 2% or more were achieved in samples having a lower value of the matrix toughness while tensile strains of around 1.6% were recorded in higher toughness ECC. Moreover, when values for the frictional bond were compared, results showed that the 0.35 ECC has slightly less frictional bond strength (1.61) than the 0.3 ECC (2.1). This decrease

in bond strength is possibly due to the higher w/b ratio of the 0.35 ECC sample but the decrease did not affect performance as it is usually accompanied with a significant matrix toughness decrease which explains why the 0.35 ECC sample performed better than the 0.3 ECC. Furthermore, when the 14 days strain results are compared to the 7 days strain results, it becomes obvious that tensile strain is increasing with age for all samples. The following graph shows the 7 days strain capacity of the same ECC samples:

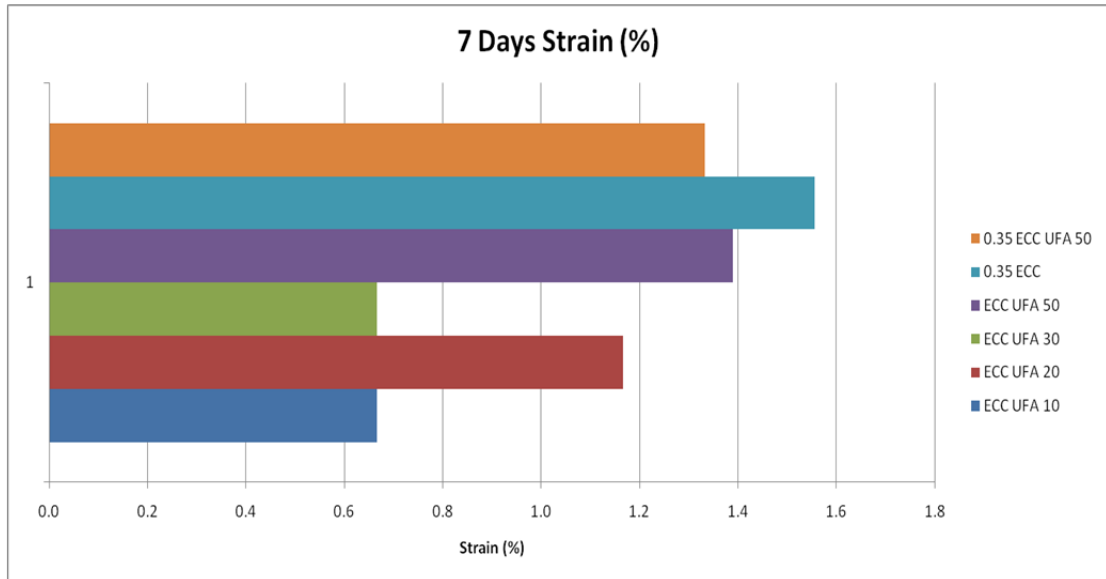


Figure 23: Seven days tensile strain of all the tested ECC mixtures.

This phenomenon can be explained theoretically or qualitatively by looking at the micromechanics design concepts of ECC. As the samples are gaining strength, the matrix toughness and the frictional bond of the fiber/matrix interface are increasing. Therefore it is theorized that as the samples age, the contribution of the increase in frictional bond strength to the increase in tensile strain capacity is higher than the contribution of the increase in matrix toughness to the decrease in tensile strain capacity. If that is the case, the assumption of higher strain capacity with age is highly justifiable. Micromechanics can be used to test this hypothesis, and that is by calculating the increase in frictional bond strength and comparing it with the increase in matrix toughness through the energy balance equations. This called for the calculation of the frictional bond. Results of the frictional bond variation with age show that the bond is increasing with age. However, unfortunately the matrix toughness variation with age cannot be calculated but it is widely accepted and known that the matrix toughness increases with age. Usually the matrix toughness is found by

testing. Therefore, this point can be proven quantitatively in a later research as it is out of the scope of this project. Furthermore, in standard ECC it is known that strain capacity increases almost linearly with frictional bond strength [26]. Therefore, strain capacity was plotted versus the frictional bond strength to verify if this phenomenon applies to the ECC samples produced in this research. The following graph shows the variation of strain capacity with respect to the fiber/matrix interface frictional bond:

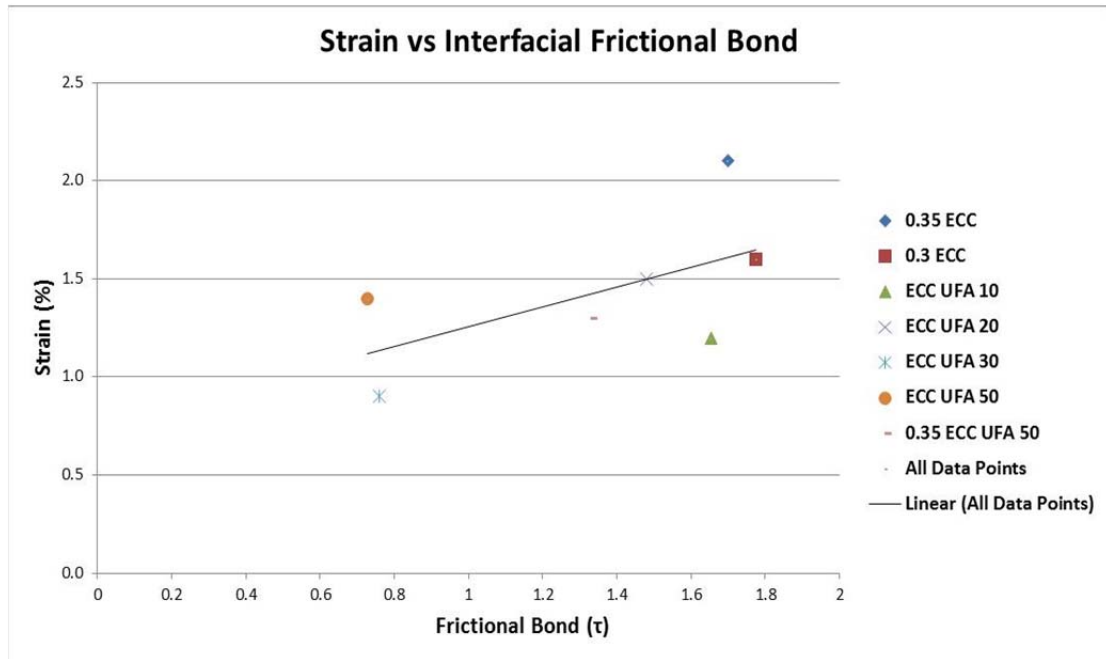


Figure 24: Plot of tensile strain variation with interfacial frictional bond.

From the reverse frictional bond calculations, it can be noticed that the strain capacity of ECC is increasing when the frictional bond of the fiber/matrix interface increases. However, this high bond value was not observed in polyethylene ECC before. It was only observed with PVA-ECC (Poly Vinyl-alcohol ECC). The reason behind the high bond strength could be the good particle packing which resulted from proportioning mixes based on mortar flow table tests. Also the relatively high tensile and compressive strength of the matrix is contributing to the frictional bond. These bond values are an estimate and do not represent the real frictional bond values. To find out the real frictional bond, fiber pullout tests should be conducted on this type of matrix.

4.1.3 The effect of ultra-fine fly ash on ECC:

Regarding the mixes containing fly ash, it is theorized that the matrix toughness did not increase when the fly ash was added as the fly ash did not complete its hydration yet. Ultra-fine fly ash is known to produce very desirable characteristics when added to normal concrete however it needs 56 days and sometimes 90 days to complete its hydration. Therefore a preliminary analysis of the mixes containing fly ash suggests that the un-hydrated fly ash particles are acting as defects inside the matrix and are causing lower matrix toughness in UFFA ECC. When the fly ash content reaches 50%, there are too many defects in the matrix which causes a major fracture and a drop in the strain capacity. Because of this phenomenon, the effect of fly ash on strain cannot be concluded based on 14 days results. A future research will test UFFA ECC at 56 days to find out the proper effect of UFFA on the hardened properties of ECC. However, ultra-fine fly ash had an interesting effect on the amount of High Range Water Reducer (HRWR) used in the mixtures. The dosage of the HRWR in each mixture was determined visually by adding it until the desired fresh ECC characteristics were judged as acceptable based on past experience. The following table shows how ultra-fine fly ash decreased the HRWR dosage:

Table 15: HRWR dosage with increasing UFFA content.

UFFA Content in 0.3 W/B ECC:	HRWR Dosage (Liters/m ³)
0.3 ECC (NO UFFA)	2.5 – 3
0.3 UFFA 10%	2
0.3 UFFA 20%	1.8
0.3 UFFA 30%	1.5
0.3 UFFA 50%	1.2
UFFA Content in 0.35 W/B ECC:	HRWR Dosage (Liters/m ³)
0.35 ECC (NO UFFA)	1.2
0.35 UFFA 50%	None

The specific gravity of the HRWR is 1.07 which means that these numbers are almost equivalent to numbers in Kg/m³. The highest value in the table above is about 3 liters per cubic meter and that was for normal non-standard ECC which does not contain UFFA. The value 3 liters per cubic meter is very low and is by far one of the lowest dosages of HRWR used to make ECC reported in literature. When UFFA is added, the HRWR dosage starts to decrease. As more UFFA is being added, the HRWR dosage keeps on decreasing until it reaches 1.2 liters per cubic meter at 50% UFFA. Moreover, if the water to binder ratio is increased to 0.35 when 50% UFFA is

used, the mixture becomes very workable without adding any water reducer. The better particle packing of the mixes due to proportioning based on mortar flow table test results is also playing a role in decreasing the water demand of the mixtures. However this procedure was used in all of the mixtures listed in the previous table. Therefore the table shows only the contribution of UFFA to the HRWR demand.

4.1.4 Comparison with data in the literature:

As mentioned earlier, ECC was first thought to be a cementitious material that can be made only with sand. However, researchers proved that ECC can be made with different types of aggregates such as crushed sand which has a maximum particle size of 2.38 [24]. Yet this reduced the strain capacity of ECC from 5% to 2% but a 1% regain in strain was achieved by adding mineral admixtures such as fly ash [34] [24]. The ECC made with aggregates which achieved 2% strain was an ECC having a compressive strength of 60 MPa. Also it was made with an aggregate to binder ratio of 0.36. They were able to enhance its strain capacity to 3% by replacing large amounts of cement with fly ash. However, a significant drop in strength resulted from the addition of fly ash. This drop in strength is considered a matrix toughness decrease and that could be the reason for the enhanced strain capacity. Now when their data is compared to the data in the current research, both the strength and the aggregate to binder ratio should be taken into consideration as they are playing a role in increasing the matrix toughness of the ECC mixtures in this research. The compressive strength of ECC mixtures produced in this research reached 83 MPa. Also, an aggregate to binder ratio of 0.8 was used. This means that samples produced in the current research contain twice the amount of aggregates that can be found in samples produced by the previous research. This alone should be considered an improvement as the current samples achieved an average strain of 1.9% at 14 days. This is expected to increase to reach 2.5% on 28 days. The main factor contributing to this improvement is the better particle packing of the aggregates in the matrix which included the use of two types of aggregates. Also by using dune sand as 45% of the total aggregates, only 55% of the aggregates are contributing to the matrix toughness increase which usually lowers the strain capacity. The following is a comparison between stress / strain diagrams produced in previous research and the current stress strain data.

Data produced by previous research:

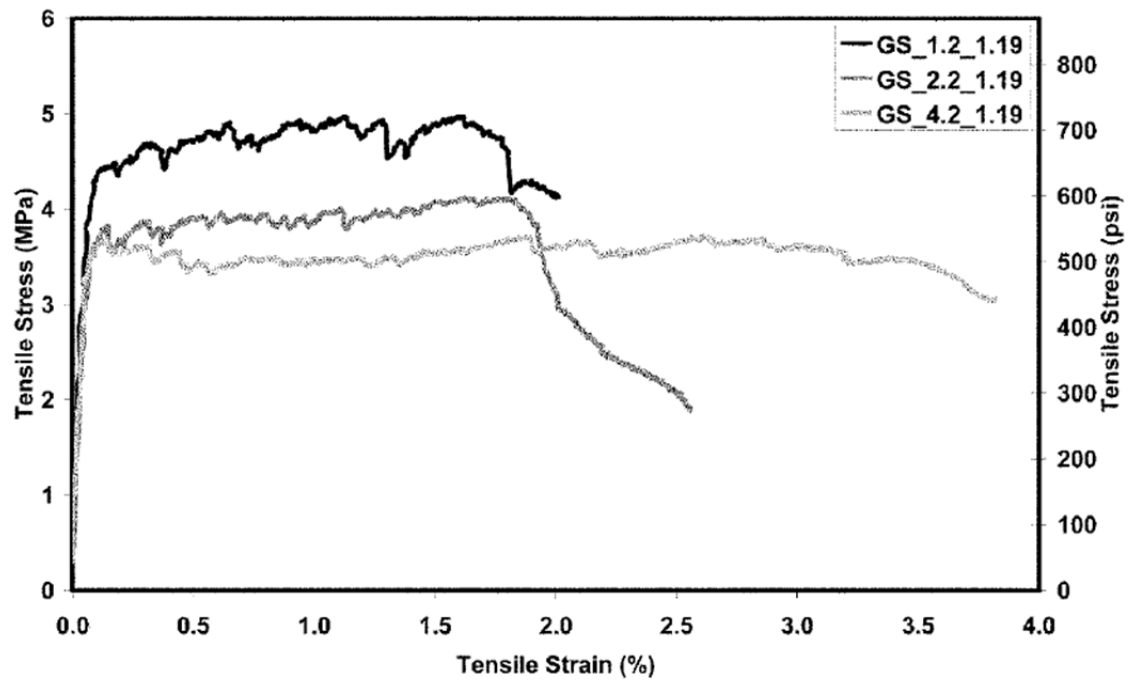


Figure 25: Tensile stress versus strain diagrams from previous research on ECC made with aggregates (dolomitic limestone) [24].

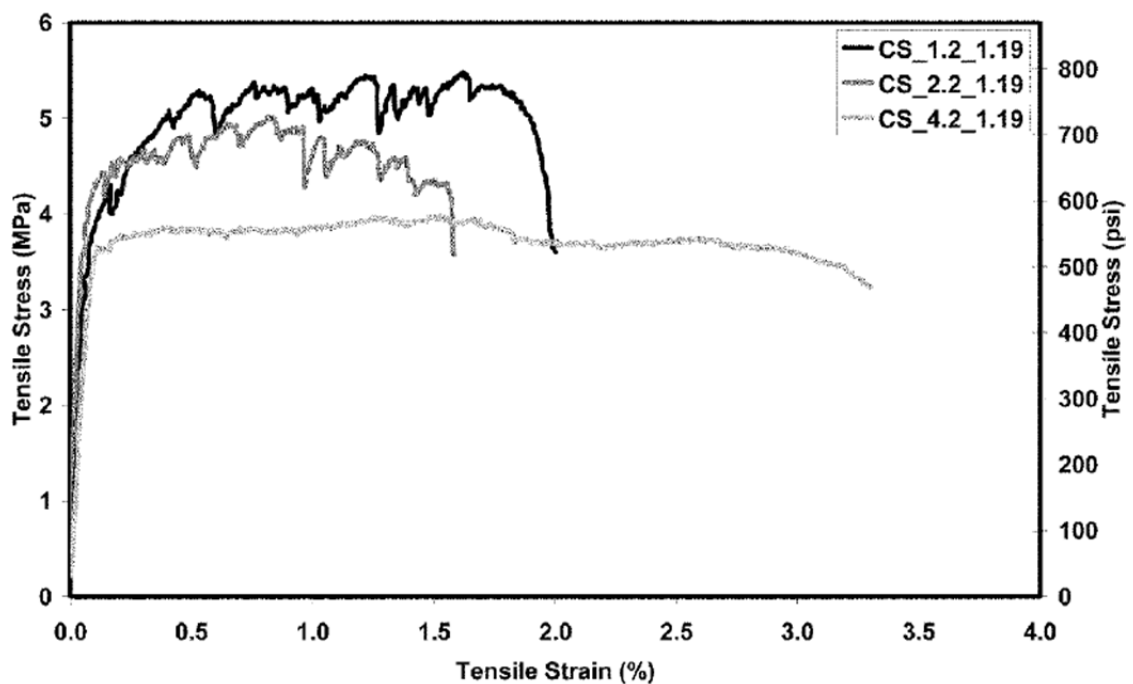


Figure 26: Tensile stress versus strain diagrams from previous research on ECC made with aggregates (gravel sand) [24].

Data produced in this research:

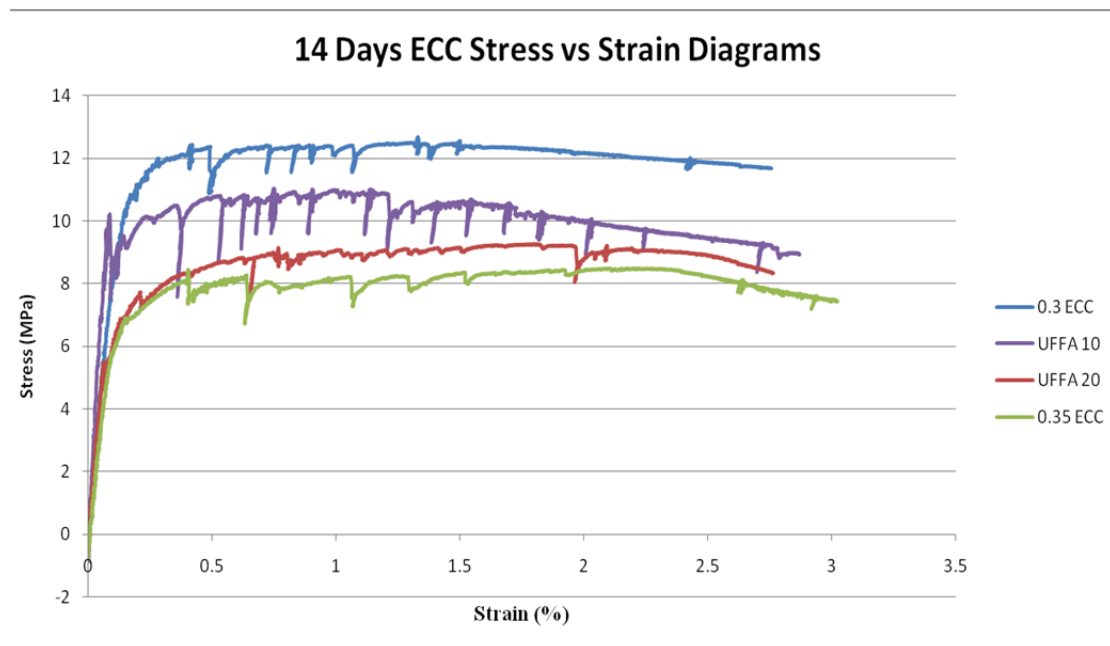


Figure 27: Tensile stress versus strain diagrams of several ECC samples in the current research.

From the above data, it is clear that ECC containing 1.73 mm aggregates with an aggregate to binder ratio of 0.8 can achieve a strain of 2%. As concluded earlier, the 0.35 ECC is expected to have a lower toughness than the rest of the samples and therefore performed better. It reached a maximum strain capacity of 2.5%. Also, the UFFA 20 which has a lower tensile strength and thus lower toughness achieved a strain capacity of 2%. However, higher strength samples such as 0.3 ECC and UFFA 10 had a strain capacity of 1.7% and 1.6% respectively. The above data is for samples which performed well in terms of multiple cracking. Some samples did not perform as well as these because of a gripping problem with the tension machine. This problem is discussed in the failure modes and errors section of the thesis. The following graph shows the 14 days strain capacity of each of the samples individually:

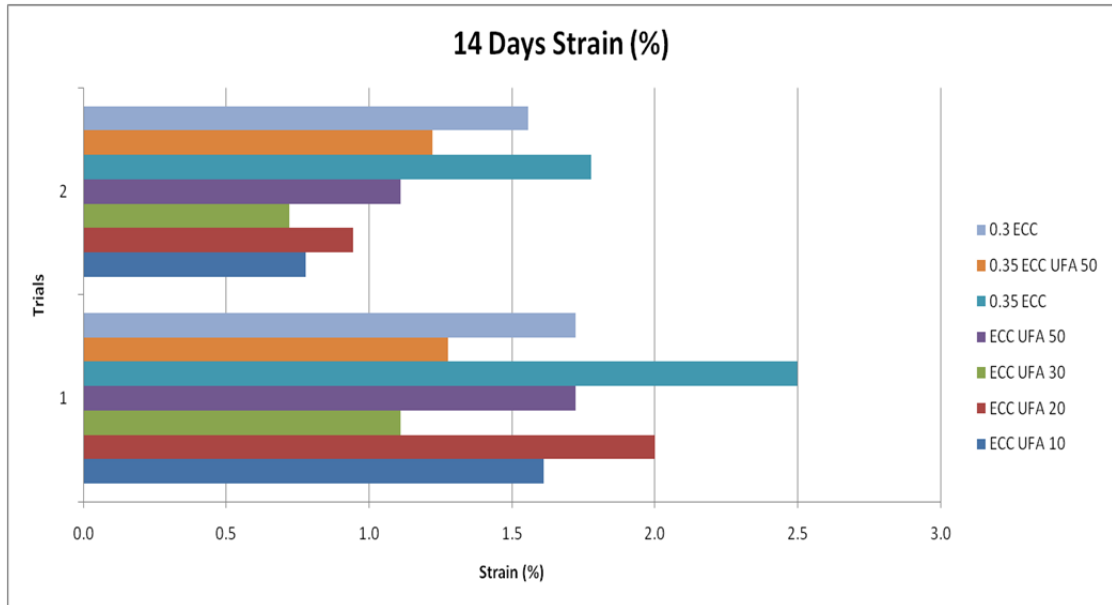


Figure 28: 14 days tensile strain results of individual ECC samples tested in this research.

From the above graph, it is obvious that all samples labeled as trail 1, performed better than samples labeled as trial 2. Therefore, there should be something hindering the performance of samples in trial 2. Actually, several factors are leading to this occurrence. One of the factors is the problem with the machine grips which will be discussed in the next section. The other factor could be the fiber distribution inside the samples. However if it was a fiber distribution problem, then things should be random. A trend as obvious as the one shown in the previous graph cannot be created by coincidence. Therefore the contribution of the fiber distribution to the variation in strain capacity is thought to be less than the contribution of the gripping problem to it.

4.1.5 Analytical Prediction:

Micromechanics can be used to validate the results of this research. ECC micromechanics principles which were discussed earlier state that a PSH Energy index of 3 is required to guarantee saturated multiple cracking in a composite. In a previous research, it was shown that the multiple cracking behavior of a composite shows up when the PSH Energy index of the composite is greater than 1. The PSH Energy index can be calculated from equation 2.11 mentioned earlier. Equation 2.11 requires the values of both J_{tip} and J_b' . J_{tip} can be found from equation 2.7 while J_b' from equation 2.13. Knowing that the frictional bond strength of polyethylene in

mortar is usually between 0.6 and 0.8 MPa, various values for the bond strength were chosen over an interval between 0.6 and 1.6 MPa. Then the complementary energy J_b' was calculated for several bond strengths in that interval. Also, knowing that the possible range of the matrix toughness of mortar is usually depicted between 0 and 1 MPa/m², several values of the matrix toughness were chosen from that interval. Then the crack tip toughness J_{tip} was calculated for each chosen matrix toughness value. In this process, a composite elastic modulus of 22 GPa was assumed. After that, the calculated values of J_b' and J_{tip} for the chosen frictional bond and matrix toughness intervals were used to calculate the PSH Energy Index at each point and plot the graph below.

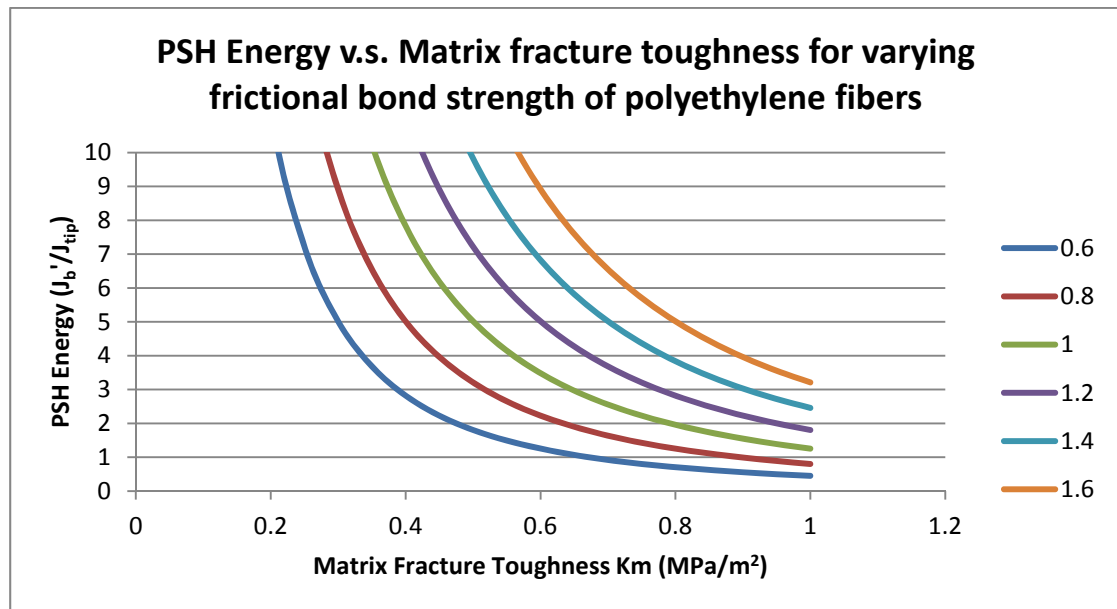


Figure 29: PSH Energy Index for all possible matrix toughness and frictional bond values.

Previous research showed that a PSH Energy index of 3 guarantees that saturated multiple cracking will happen in a composite. This graph says that in order to achieve a PSH Energy index of 3, one must aim for matrix toughness between 0.4 and 0.6 MPa/m² if the fiber frictional bond strength was between 0.6 and 0.8. More importantly, this graph says that if the bond strength is as high as 1.4, the composite should achieve saturated multiple cracking and thus strain hardening regardless of the matrix toughness. In this research, the best sample had an estimated frictional bond value as high as 1.6 while poorly performing samples had estimated bond values of around 0.6 to 0.7. The graph clearly validates the results of this research. However, the possibility of achieving a bond as high as 1.6 is still controversy. Fiber pullout

tests are needed to solve this controversy. Considering how well the above predictions fit the data, and the fact that the bond values listed before are estimates, one can easily doubt that the bond values were overestimated. Reasons for this overestimation of bond values could be the unknown snubbing factor of the polyethylene fibers as no other research mentioned the snubbing factor of polyethylene. Other factors contributing to the overestimation of the frictional bond strength could be an inaccuracy in measuring the tensile strength of the ECC samples.

4.2 Failure modes and possible errors affecting the results:

4.2.1 Uniform distribution of fibers in the matrix:

For ECC to work, a uniform distribution of fibers in the matrix is vital. A water / Binder ratio of 0.3 or less is recommended by research to achieve a good fiber distribution in the matrix [29]. That is why most ECC found in research is being made using a 0.27 Water / Binder ratio. However in this research, a water / binder ratio of 0.3 was used. This water binder ratio of 0.3 is considered the upper limit of good rheology but it was chosen in order to offset the possible increase of toughness due to the use of aggregates and the increased aggregate to binder ratio (0.8). Also, an enhanced mixing method proposed by previous research was used in order to improve the fiber distribution in the matrix [33]. Moreover, this method is commonly used to improve the fiber distribution in mixtures having higher water / binder ratio such as 0.35. Since this mixing method was used for all samples prepared in this research, and since the water / binder ratio was selected on the basis of achieving good rheology which equals a good fiber distribution, then it can be said that the contribution of the varying fiber distribution to the varying mechanical performance of samples in this research is very low. Also as mentioned earlier, fibers were dispersed by air pressure before being added to the matrix. This further decreases the probability of varying fiber distribution to interfere with the results. Furthermore, some samples were cut in several places and it was observed by the naked eye that fibers were well distributed over the cut section.

4.2.2 Aggregate size:

Aggregates having a large size are known to increase the toughness of a matrix. For instance, when a crack is propagating in mortar containing sand only, it faces less

resistance than when the same crack is propagating in mortar containing aggregates. This happens because when the crack tip meets an aggregate, it has two options. Either break the aggregate or continue to propagate around it. If the aggregate is weak then the first scenario will happen. However if the aggregate is strong, the crack will be forced to travel around it. Yet, in both cases, the crack needs much more energy to propagate when compared to a situation where the crack meets a much smaller sand particle instead of an aggregate particle. This phenomenon usually lowers the strain capacity of ECC containing aggregates. Therefore it is theorized that if the aggregates in this ECC are replaced by sand, the strain capacity will rise to 5% if not more.

4.2.3 Machine Gripping:

In this research, it was observed that some samples were performing much better than others. Also, it was observed that for the samples performing well, multiple cracking occurred over the entire length of the sample. However, for the samples performing poorly, multiple cracking was forced to happen next to the lower grip of the tensile testing machine. The following pictures depict the difference between the two set of samples:



Figure 30: Bad samples (cracks are seen next to the grips only).



Figure 31: Good samples (tiny micro-cracks distributed over the sample length).



Figure 32: Good sample top view.



Figure 33: Good sample top view (zoomed in at the cracks area).

The previous pictures show that in the samples with low strain capacity, major multiple cracking happened only next to the grips while some very small minor cracks happened over the length of the samples. However, in the case of the good performing samples, most multiple cracking started in the middle with little or no cracking next to the grips. The second picture above shows how the cracks are away from the grips with some cracks or none of the cracks next to the grips. While the first picture shows

that almost 75 % of the sample was intact or suffered from very small cracks which are not visible in this picture because they are too small to be seen by a camera picture. The two types of failure were observed in all samples not just in the seven samples shown in the pictures. This led to the conclusion that the machine grips are exerting a high compressive force on all of the samples which is lowering the strain capacity of the samples. Unfortunately, the gripping force of this type of machine cannot be adjusted. Nevertheless, the strain capacity observed in this research is good enough, when considering non-standard ECC which contains aggregates. Therefore, it is suggested that in a later research, another machine should be used to accurately predict the strain capacity of this type of samples. Based on this observation, it is obvious that the strain capacity of all samples should increase if a better machine is used. Also since tension testing is considered one of the hardest tests to be accurately done, especially on concrete or ECC, there are other errors which might affect the results. However these errors are not considered major. The following paragraph will discuss other possible errors.

4.2.4 Testing Errors:

The following are considered errors that might be contributing to some of the variation in the results:

- a. Difference in the level of the epoxy which was used to stick aluminum plates on the samples.
- b. Alignment of ECC and handling or gripping during the tension test.
- c. Increase / decrease in thickness of the samples due to mold defects.

The highest reported increase in thickness which occurred in one of the ECC samples was 1.4 mm. Also, the highest value of thickness loss was 0.4 mm. The alignment of the samples during the tension test was done using the naked human eye.

Chapter 5: Summary, Conclusions, and Future Research

5.1 Summary

In the beginning, the fracture mechanics and the micromechanics used to develop Engineered Cementitious Composites were reviewed and summarized. Then, micromechanical parameters linking material microstructures to material properties and thus structural applications were addressed and emphasized. From the review, it is clear that two major criteria must be fulfilled in order to achieve strain hardening in discontinuous random fiber reinforced cement composites. Thus those micromechanical models were used to guide the material design of ECC. Nevertheless, the efficient and effective design of ECC requires tailoring of the fiber, matrix, and fiber/matrix interface. Regarding the interface, both the frictional bond and the chemical bond should be tailored as it significantly affects the complementary energy and strain hardening behavior. Also, fiber characteristics and type are extremely important and are considered at the core of the ECC design theory. Fiber tailoring is important because the fiber tensile strength, fiber length, fiber diameter and fiber elastic modulus can affect the critical volume fraction required for strain hardening and thus affect the cost of the composite. Also because each fiber type has a different interface tailoring requirement, some of the techniques mentioned in the literature review were used while others were not. It should be mentioned that a wide range of fiber interface strengthening mechanisms other than interface densification by particle packing are available such as surface treatment by plasma. However, these methods are complicated and are not available everywhere in the world. Therefore interface densification by increasing the matrix particle packing which is considered one of the easiest methods for tailoring the fiber interface was used in this research. In addition, other aspects that need to be tailored are the matrix parameters which include the matrix toughness and matrix flaw size. Since the matrix flaw size is random in nature and methods of altering the flaw size are usually difficult, the focus was on tailoring the matrix toughness. The matrix toughness can be modified by changing the type and size of aggregate, the aggregate to binder ratio, the water to binder ratio, or by the addition of mineral admixtures. In this research the matrix toughness was controlled using the water to binder ratio, the aggregate to binder ratio, and by the addition of ultra-fine fly ash which is a mineral admixture. With the help of the previous toughness modification methods, the matrix toughness was kept low

in order to decrease the crack tip toughness (J_{tip}) and make it easier to achieve strain hardening behavior. However, in this research, the focus was more on tailoring the fiber/matrix interface through particle packing rather than tailoring the matrix toughness. This is due to the fact that higher interfacial bond strengths which result from a better matrix particle packing can accommodate higher matrix toughness. This result was shown to be theoretically correct in figure 28. Furthermore, good rheological control i.e. viscosity and workability control of ECC is considered important for achieving a uniform distribution of the fibers in the cement matrix. In this research, the rheological control was achieved by modifying the water to binder ratio, the HRWR dosage, and by enhancing the mixing sequence. Finally, careful attention to all the parameters discussed in this summary and their interaction with each other was practiced in order to attain ECC samples having a good mechanical performance. The lack of attention to any of these parameters might result in a low strain capacity. ECC is still considered a new material and further research should be done to quantify and confirm the effect of each parameter or new and unstudied parameters on the behavior of the material. Therefore this study is considered important since it investigates the effects of new parameters on the mechanical performance of a non-standard type of ECC.

5.2 Conclusions & Future Research:

5.2.1 Conclusions:

After the results were analyzed, the following conclusions were made:

1. ECC can be made with aggregates and with twice the amount of aggregate or sand in standard ECC.
2. Strain capacities of 1.9% on average and up to 2.5% were achieved at 14 days by the newly created non-standard ECC.
3. ECC with aggregates created in this research achieved an average tensile strength of 8 MPa and a compressive strength of 82 MPa.
4. Particle packing of ECC matrices can enhance the polyethylene fiber / matrix interfacial bond to a great extent.
5. Higher matrix toughness can be accommodated if the frictional bond of polyethylene is increased.

6. A large amount of cement can be replaced with Fly Ash & UFFA which greatly enhances the fresh properties and the greenness of ECC.
7. Local aggregates such as crushed limestone and dune sand can be used to produce ECC while preserving its good mechanical properties.

5.2.2 Discussion of Conclusions and Future Research:

Previous research confirmed that it is possible to produce ECC having good mechanical performance even when aggregates or larger sand particles are used [22]. Therefore this research sought to incorporate a larger amount of aggregates having a larger aggregate size to create a non-standard ECC that is expected compete with the previous non-standard ECC. Strain capacities up to 2.5 % were achieved by this newly created non-standard ECC. On average a strain of 1.9% was achieved. However, these results are only 14 days results and the strain capacity is expected to increase a little more at 28 days. The benefits of adding aggregates in a large amount include reducing cement volume, better drying shrinkage and creep resistance, better workability, less cost and less carbon footprint. Another finding of this research is that the particle packing of ECC matrices can enhance the frictional fiber/matrix interface bond to a great extent. Previous research mentioned that the weak zone around the fiber which causes the bond to be low can be enhanced by particle packing [26]. This means a better particle packing density is favorable for ECC however they did not quantify or attempt to study its effects [26]. Also, previous research mentioned that a large amount of cement can be replaced by fly ash while enhancing the mechanical performance. Therefore, a better class of fly ash known as ultra-fine fly ash was used in this research. UFFA did enhance the fresh ECC properties however accurate conclusions are yet to be made regarding its effect on the mechanical performance of ECC. Yet again, the effect of fly ash is well documented by more than six researches which were previously referred to in this thesis. All of these researches agree that fly ash enhances the hardened properties and the mechanical performance of ECC. Therefore it is expected that even at 50% cement replacement by ultra-fine fly ash, ECC with good performance can be produced. Moreover, local aggregates available in the UAE were successfully incorporated in the ECC mixtures without hindering any of its mechanical properties. The only thing that was purchased from foreign countries was the fiber because no competing fibers were found in the UAE market.

Furthermore, the tensile strain and strength results of ECC containing aggregates up to 1.7mm in size and an aggregate to binder ratio of 0.8 were better than results produced in a previous research having an aggregate to binder ratio of 0.4. It was theorized that the increased matrix particle packing was the reason behind the better results. Finally, this research opened the door for a significant amount of research on ECC. Future research can focus on enhancing the fiber / matrix interfacial bond through particle packing in order to achieve better mechanical performance. Also the bond can be further enhanced by particle packing the cement paste, or by using supplementary cementitious materials such as condensed silica fume. As the cement paste constitutes almost 50% of this non-standard ECC, particle packing the cement paste is expected to greatly enhance the results. In this research particle packing was done on aggregates only. These suggestions were not tested yet on this type of non-standard ECC. However, a future research will focus on particle packing the cement paste and will study the effect of Ultra-fine fly ash on the tensile strength of ECC. Moreover, other types of aggregates available in the UAE can be tested. A wide range of parameters that are usually studied in durability tests such as rapid chloride penetration can be performed on this non-standard ECC. In addition, a fiber type that is comparable to polyethylene or PVA may become available and that alone will further enhance the significance of this research.

Works Cited

- [1] V. C. Li, "Large Volume, High-Performance Applications of Fibers in Civil Engineering," *Journal of Applied Polymer Science*, vol. 83, no. 3, pp. 660-686, 2002.
- [2] V. C. Li, "Engineered Cementitious Composites (ECC) - Tailored Composites Through Micromechanical Modeling," in *Fiber Reinforced Concrete: Present and the Future*, Montreal, 1998, pp. 64-97.
- [3] V. C. Li and H. C. Wu, "Conditions for Pseudo Strain-Hardening in Fiber Reinforced Brittle Matrix Composites," *Applied Mechanics Reviews*, vol. 45, no. 8, pp. 390-398, 1992.
- [4] V. C. Li and C.K.Y. Leung, "Steady State and Multiple Cracking of Short Random Fiber Composites," *Journal of Engineering Mechanics*, vol. 118, no. 11, pp. 2246-2264, 1992.
- [5] V. C. Li, S. Wang, and C. Wu, "Tensile Strain-Hardening Behavior of Polyvinyl Alcohol Engineered Cementitious Composite (PVA-ECC)," *ACI Materials Journal*, vol. 98, no. 6, pp. 483-492, 2001.
- [6] V. C. Li, C. Wu, S. Wang, A. Ogawa, and T. Saito, "Interface Tailoring for Strain-Hardening Polyvinyl Alcohol-Engineered Cementitious Composite (PVA-ECC)," *ACI Materials Journal*, vol. 99, no. 5, pp. 463-472, 2002.
- [7] E. Yang, Y. Yang, and V. C. Li, "Use of High Volumes of Fly Ash to Improve ECC Mechanical Properties and Material Greenness," *ACI Materials Journal*, vol. 104, no. 6, pp. 620-628, 2007.
- [8] S. Wang and V. C. Li, "Engineered Cementitious Composites with High-Volume Fly Ash," *ACI Materials Journal*, vol. 104, no. 3, pp. 233-241, 2007.
- [9] E. Yang and V. C. Li, "Rate Dependence in Engineered Cementitious Composites," in *International RILEM Workshop on High Performance Fiber Reinforced Cementitious Composites in Structural Applications*, 2006, pp. 83-92.
- [10] M. Maalej, Quek. S., and J. Zhang, "Behavior of Hybrid Fiber Engineered Cementitious Composites Subjected to Dynamic Tensile Loading and Projectile Impact," *Journal of Materials in Civil Engineering*, pp. 143 - 152, April 2005.
- [11] J. Zhang, M. Maalej, and S. T. Quek, "Performance of Hybrid-Fiber ECC Blast/Shelter Panels Subjected to Drop Weight Impact," *Journal of Materials in Civil Engineering ASCE*, pp. 855-863, October 2007.
- [12] V. C. Li, "From Micromechanics to Structural Engineering-the Design of Cementitious Composites for Civil Engineering Applications," *Structural Engineering/Earthquake Engineering*, vol. 10, no. 2, pp. 1-34, 1994.

- [13] V. C. Li, "On Engineered Cementitious Composites (ECC) A Review of the Material and Its Applications," *Journal of Advanced Concrete Technology*, vol. 1, no. 3, pp. 215-230, 2003.
- [14] E. Yang, S. Wang, Y. Yang, and V. C. Li, "Fiber-Bridging Constitutive Law of Engineered Cementitious Composites," *Journal of Advanced Concrete Technology*, vol. 6, no. 1, pp. 181-193, 2008.
- [15] Z. Lin, T. Kanda, and V. C. Li, "On Interface Property Characterization and Performance of Fibe-Reinforced Cementitious Composites," *Concrete Science and Engineering*, vol. 1, no. 3, pp. 173-184, 1999.
- [16] E. Yang and V. C. Li, "Numerical Study on Steady-State Cracking of Composites," *Composites Science and Technology*, vol. 67, no. 2, pp. 151-156, 2007.
- [17] M. Maalej, T. Hashida, and V. C. Li, "Effect of Fiber Volume Fraction on the Off-Crack-Plane Fracture Energy in Strain-Hardening Engineered Cementitious Composites," *Journal of the American Ceramic Society*, vol. 78, no. 12, pp. 3369-3375, 1995.
- [18] V. C. Li and M. Maalej, "Toughening in Cement Based Composites. Part I: Cement, Mortar, and Concrete," *Cement and Concrete Composites*, vol. 18, no. 4, pp. 223-237, 1996.
- [19] V. C. Li and M. Maalej, "Toughening in Cement Based Composites. Part II: Fiber Reinforced Cementitious Composites," *Cement and Concrete Composites*, vol. 18, no. 4, pp. 239-249, 1996.
- [20] E. Yang and V. C. Li, "Strain-Hardening Fiber Cement Optimization and Component Tailoring by Means of a Micromechanical Model," *Construction and Building Materials*, vol. 24, no. 2, pp. 130-139, 2010.
- [21] P. Kabele, "New Developments in Analytical Modeling of Mechanical Behavior of ECC," *Journal of Advanced Concrete Technology*, vol. 1, no. 3, pp. 253-264, 2003.
- [22] V. C. Li, H. C. Wu, M. Maalej, D. K. Mishra, and T. Hashida, "Tensile Behavior of Cement-Based Composites with Random Discontinuous Steel Fibers," *Journal of the American Ceramic Society*, vol. 79, no. 1, pp. 74-78, 1996.
- [23] V. C. Li, D. K. Mishra, and H. C. Wu, "Matrix Design for Pseudo Strain-Hardening Fiber Reinforced Cementitious Composites," *Journal of Materials and Structures*, vol. 28, no. 184, pp. 586-595, 1995.
- [24] M. Sahmaran, M. Lachemi, M. A. Khandaker, R. Ranade, and V. C. Li, "Influence of Aggregate Type and Size on Ductility and Mechanical Properties of Engineered Cementitious Composites," *ACI Materials Journal*, vol. 106, no. 3, pp. 308-316, 2009.

- [25] C. Redon et al., "Measuring and Modifying Interface Properties of PVA Fibers in ECC Matrix," *Journal of Materials in Civil Engineering*, vol. 13, no. 6, pp. 399-406, 2001.
- [26] V. C. Li, H. C. Wu, and Y. Chan, "Effect of Plasma Treatment of Polyethylene Fibers on Interface and Cementitious Composite Properties," *Journal of the American Ceramic Society*, vol. 79, no. 3, pp. 700-704, 1996.
- [27] V. C. Li and H. Stang, "Interface Property Characterization and Strengthening Mechanisms in Fiber Reinforced Cement Based Composites," *Advanced Cement Based Materials*, vol. 6, no. 1, pp. 1-20, 1997.
- [28] J. Zhou et al., "Development of Engineered Cementitious Composites with Limestone Powder and Blast Furnace Slag," *Journal of Materials and Structures*, vol. 43, no. 6, pp. 803-814, 2010.
- [29] E. Yang, M. Sahmaran, Y. Yang, and V. C. Li, "Rheological Control in Production of Engineered Cementitious Composites," *ACI Materials Journal*, vol. 106, no. 4, pp. 357-366, 2009.
- [30] G. Fischer and V. C. Li, "Design of Engineered Cementitious Composites (ECC) for Processing and Workability Requirement," in *BMC-7*, Poland, 2003, pp. 29-36.
- [31] J. K. Kim, J. S. Kim, G. J. Ha, and Y. Y. Kim, "Tensile and Fiber Dispersion Performance of ECC (Engineered Cementitious Composites) Produced with Ground Granulated Blast Furnace Slag," *Cement and Concrete Research*, vol. 37, no. 7, pp. 1096-1105, 2007.
- [32] A. Bentur et al., "Fiber-Matrix interfaces," in *Pre-Proceedings 2nd International Workshop 'High Performance Fiber Reinforced Cement Composites (HPF-RCC-95)*, Ann Arbor, Michigan, 1995, pp. 139-182.
- [33] J. Zhou et al., "Improved Fiber Distribution and Mechanical Properties of Engineered Cementitious Composites by Adjusting the Mixing Sequence," *Cement and Concrete Composites*, vol. 34, no. 3, pp. 342-348, 2012.
- [34] M. Sahmaran, H. E. Yucel, S. Demirhan, M. T. Arik, and V. C. Li, "Combined Effect of Aggregate and Mineral Admixtures on Tensile Ductility of Engineered Cementitious Composites," *ACI Materials Journal*, vol. 109, no. 6, pp. 627 - 637, November 2012.
- [35] K. Wille, A. E. Naaman, and G. J. Parra-Montesinos, "Ultra-High Performance Concrete with Compressive Strength Exceeding 150 MPa (22 Ksi): A Simpler Way," *ACI Materials Journal*, vol. 108, no. 1, pp. 46-54, February 2011.

Appendix

Table 16: Tensile strain and tensile strength data for all the samples at 7 days and 14 days.

			First Trial	Second Trial	First Trial	Second Trial
	Strain 7 Days (%)	Strength 7 Days (MPa)	Strain 14 Days (%)	Strain 14 Days (%)	Strength 14 Days (MPa)	Strength 14 Days (MPa)
0.35 ECC	1.6	8.58	2.5	1.8	10.60	10.83
0.35 ECC UFA 50	1.3	7.91	1.3	1.2	10.24	6.58
0.3 ECC	-	-	1.7	1.6	15.22	11.22
ECC UFA 10	0.7	8.88	1.6	0.8	8.50	12.36
ECC UFA 20	1.2	12.90	2.0	0.9	11.60	7.05
ECC UFA 30	0.7	4.20	1.1	0.7	6.04	3.51
ECC UFA 50	1.4	3.61	1.7	1.1	4.84	4.37

Table 17: Average tensile strain and tensile strength for all the samples at 7 days and 14 days.

			Average	Average
	Strain 7 Days (%)	Strength 7 Days (MPa)	Strain 14 Days (%)	Strength 14 Days (MPa)
0.35 ECC	1.6	8.58	2.1	10.72
0.35 ECC UFA 50	1.3	7.91	1.3	8.41
0.3 ECC	-	-	1.6	13.22
ECC UFA 10	0.7	8.88	1.2	10.43
ECC UFA 20	1.2	12.90	1.5	9.33
ECC UFA 30	0.7	4.20	0.9	4.77
ECC UFA 50	1.4	3.61	1.4	4.60

Table 18: Calculation of the crack tip toughness (J_{tip}) using the possible matrix toughness interval (0.1 to 1).

K_m (MPa/m ²)	J_{tip} (J/m ²)
1	45.5
0.95	41.0
0.9	36.8
0.85	32.8
0.8	29.1
0.75	25.6
0.7	22.3
0.65	19.2
0.6	16.4
0.55	13.8
0.5	11.4
0.45	9.2
0.4	7.3
0.35	5.6
0.3	4.1
0.25	2.8
0.2	1.8
0.15	1.0
0.1	0.5

Table 19: Calculation of the complementary energy J_b' using a chosen frictional bond interval (0.6 to 2.1).

τ_0	J_b'
0.6	21
0.7	28
0.8	36
0.9	46
1	57
1.1	69
1.2	82
1.3	96
1.4	112
1.5	128
1.6	146
1.7	165
1.8	185
1.9	206
2	228
2.1	251

Table 20: All possibilities of J_b' / J_{tip} for the chosen intervals of the frictional bond and the matrix toughness; it was used to plot figure 27.

	All Possibilities of J_b' / J_{tip}																		
J_b' / J_{tip}	45.5	41.0	36.8	32.8	29.1	25.6	22.3	19.2	16.4	13.8	11.4	9.2	7.3	5.6	4.1	2.8	1.8	1.0	0.5
21	0.45	0.50	0.56	0.62	0.71	0.80	0.92	1.07	1.25	1.49	1.81	2.23	2.82	3.68	5.01	7.22	11.28	20.06	45.13
28	0.61	0.68	0.76	0.85	0.96	1.09	1.25	1.45	1.71	2.03	2.46	3.03	3.84	5.01	6.83	9.83	15.36	27.30	61.43
36	0.80	0.89	0.99	1.11	1.25	1.43	1.64	1.90	2.23	2.65	3.21	3.96	5.01	6.55	8.91	12.84	20.06	35.66	80.23
46	1.02	1.13	1.25	1.41	1.59	1.81	2.07	2.40	2.82	3.36	4.06	5.01	6.35	8.29	11.28	16.25	25.39	45.13	101.55
57	1.25	1.39	1.55	1.74	1.96	2.23	2.56	2.97	3.48	4.14	5.01	6.19	7.84	10.23	13.93	20.06	31.34	55.72	125.37
69	1.52	1.68	1.87	2.10	2.37	2.70	3.10	3.59	4.21	5.01	6.07	7.49	9.48	12.38	16.85	24.27	37.92	67.42	151.69
82	1.81	2.00	2.23	2.50	2.82	3.21	3.68	4.27	5.01	5.97	7.22	8.91	11.28	14.74	20.06	28.88	45.13	80.23	180.53
96	2.12	2.35	2.62	2.93	3.31	3.77	4.32	5.01	5.89	7.00	8.47	10.46	13.24	17.30	23.54	33.90	52.97	94.16	211.87
112	2.46	2.72	3.03	3.40	3.84	4.37	5.01	5.82	6.83	8.12	9.83	12.13	15.36	20.06	27.30	39.31	61.43	109.21	245.72
128	2.82	3.13	3.48	3.90	4.41	5.01	5.76	6.68	7.84	9.32	11.28	13.93	17.63	23.03	31.34	45.13	70.52	125.37	282.07
146	3.21	3.56	3.96	4.44	5.01	5.71	6.55	7.60	8.91	10.61	12.84	15.85	20.06	26.20	35.66	51.35	80.23	142.64	320.94
165	3.62	4.01	4.47	5.01	5.66	6.44	7.39	8.58	10.06	11.98	14.49	17.89	22.64	29.58	40.26	57.97	90.58	161.03	362.31
185	4.06	4.50	5.01	5.62	6.35	7.22	8.29	9.61	11.28	13.43	16.25	20.06	25.39	33.16	45.13	64.99	101.55	180.53	406.19
206	4.53	5.01	5.59	6.26	7.07	8.05	9.24	10.71	12.57	14.96	18.10	22.35	28.29	36.94	50.29	72.41	113.14	201.14	452.57
228	5.02	5.56	6.19	6.94	7.84	8.91	10.23	11.87	13.93	16.58	20.06	24.76	31.34	40.94	55.72	80.23	125.37	222.87	501.46
251	5.53	6.13	6.83	7.65	8.64	9.83	11.28	13.09	15.36	18.28	22.11	27.30	34.55	45.13	61.43	88.46	138.22	245.72	552.86

Vita

Michel Issa Obied was born on September 14, 1989 in Safita, Syria. His family moved to the United Arab Emirates in 1991 where he grew up and graduated from Al Mawakeb School in 2006. He then joined the American University of Sharjah for his bachelors. Upon completing his bachelor degree in Civil Engineering at the American University of Sharjah in 2011, he picked up interest in concrete technology. During his bachelor studies, he trained for about a year and a half in a concrete ready mix plant under the supervision of the QA/QC manager. He has published papers related to the field of Construction Management in several conferences such as the Seventh International Structural Engineering and Construction Conference (ISEC-7) and the GIST Global Engineering, Science and Technology Conference. His Master's thesis at American University of Sharjah was under the supervision of Professor Adil Al-Tamimi.